ELSEVIER

Sedimentary Geology 102 (1996) 221–262

SEDIMENTARY GEOLOGY

The Harricana glaciofluvial complex, Abitibi region, Quebec: its genesis and implications for meltwater regime and ice-sheet dynamics

Tracy A. Brennand [1], John Shaw

Department of Geography, University of Alberta, Edmonton, Alberta, T6G 2H4, Canada

Received 14 November 1994; revised version accepted 1 June 1995

Abstract

Interlobate moraines have been defined by their relationship to adjacent landforms and sediments, with minimal reference to any genesis suggested from their own geomorphology and sedimentology. A case in point is the "Harricana interlobate moraine".

The Harricana complex, a relatively continuous, linear accumulation of glaciofluvial sediments, is investigated in terms of its geomorphology, sedimentology, stratigraphic context, and landform associations for the portion between latitudes 48°N and 50°N. The complex is narrower to the north than to the south. In the narrower northern part, better rounding and poorer preservation of less resistant clasts suggest more vigorous transport in a narrower conduit; the inverse in the wider southern part favours less vigorous flows and higher deposition rates. These inferences, together with unidirectional paleoflows towards the ice margin and the relatively continuous upslope path of the southward-widening complex, favour synchronous formation of the Harricana complex in a continuous closed conduit, beneath an ice sheet which thinned southward. Subaqueous fans and grounding-line deposits with fine gravel and sandy in-phase wave structures in the south, may have been deposited in subglacial cavities adjacent to the complex, or later deposited in reentrants in calving ice fronts.

The basic building blocks of the Harricana complex are gravel facies which indicate generally high energy, but unsteady, transport. These facies are arranged into macroforms. Composite and oblique-accretion, avalanche-bed (OAAB) macroforms are attributed to deposition by unsteady and non-uniform flows in conduit enlargements. Pseudoanticlinal macroforms were deposited in relatively narrow conduit segments of uniform width. Gravel–sand couplets register flow unsteadiness, perhaps related to variations in supraglacial meltwater supply.

The origin of the Harricana complex as a mainly synchronous subglacial landform is linked to formation of adjacent streamlined bedforms and bedrock erosional marks by meltwater outburst floods. The complex is located where the orientation of these subglacial bedforms indicate strong flow convergence. Post-flood, ice sheet collapse along this convergence zone initiated redirection of ice flow, resulting in cross-cutting striae. Later subglacial meltwater systems followed new hydraulic gradients toward this trough of thinner ice, forming a major conduit and depositing the Harricana glaciofluvial complex.

[1] Present address: Geological Survey of Canada, 601 Booth Street, Ottawa, Ont. K1A 0E8, Canada.

SSDI 0037-0738(95)00069-0

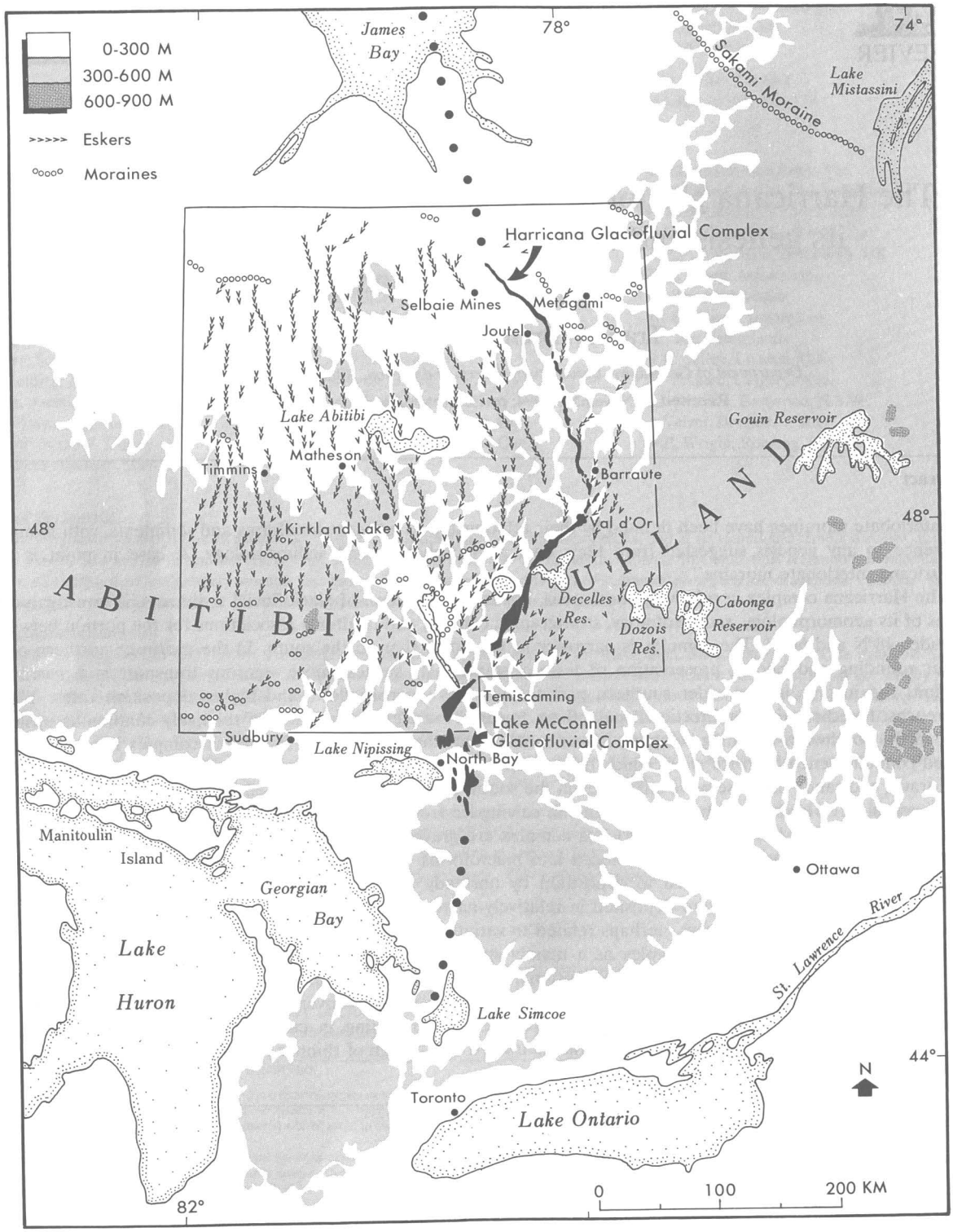
0-300 M
300-600 M
600-900 M
Eskers
Moraines
James Bay
78°
74°
Sakami Moraine
Lake Mistassini
Harricana Glaciofluvial Complex
Selbaie Mines
Metagami
Joutel
Lake Abitibi
Gouin Reservoir
Matheson
Timmins
Barraute
Val d'Or
48°
Kirkland Lake
ABITIBI
UPLAND
Decelles Res.
Dozois Res.
Cabonga Reservoir
Temiscaming
Lake McConnell Glaciofluvial Complex
Sudbury
Lake Nipissing
North Bay
Manitoulin Island
Georgian Bay
Lake Huron
Ottawa
St. Lawrence River
Lake Simcoe
44°
N
Toronto
Lake Ontario
82°
0
100
200 KM

1. Introduction

So-called interlobate moraines have been identified in Finland (e.g., Aario, 1977; Punkari, 1980) and Canada (e.g., Duckworth, 1979; Veillette, 1986; Dredge and Cowan, 1989). They are broad complexes of mainly sand and gravel, arranged in almost continuous ridges and irregular mounds (cf. Punkari, 1980). Their interlobate interpretation rests on the evidence of converging striae, their relationship with arcuate end moraines marking the margins of lobes, and their position relative to esker networks and streamlined bedforms that are said to record lobate flow. As well, the analyses of till geochemistry and pebble lithology indicate lobate dispersion patterns (e.g., Kaszycki and DiLabio, 1986; Veillette, 1989).

There are few detailed sedimentologic and geomorphologic studies of interlobate moraines themselves in the context of surrounding landforms and sedimentary and stratigraphic sequences. Yet such research is essential if we are to understand their regional significance. For this reason, we present a detailed geomorphologic and sedimentologic study of a 250 km stretch of the "Harricana interlobate moraine" (cf. Veillette, 1986), between latitudes 48°N and 50°N, in the Abitibi region of Quebec, Canada (Fig. 1).

Interlobate moraines are generally assumed to have been formed time-transgressively (e.g., Dyke and Prest, 1987). However, in our preliminary investigations of the Harricana complex we recognized sedimentary facies, facies architectures and facies associations similar to those in south-central Ontario eskers, inferred to have been deposited synchronously in subglacial conduits (Brennand, 1994). This comparison raised the possibility that the Harricana complex was also formed synchronously rather than time-transgressively. The two possibilities—piecemeal deposition and simultaneous creation of the complex over its whole length—hold major consequences for our understanding of deglacial processes (how and when?) of large ice sheets. With these two alternatives in mind, we aim to elucidate the genesis and hydrology of the Harricana complex with a view to their implications for ice-sheet dynamics. Our observations and interpretations bring into question, not only piecemeal deposition, but also the interlobate nature of this landform. Consequently, we refer to the Harricana glaciofluvial complex, rather than the Harricana interlobate moraine.

2. The Harricana glaciofluvial complex

The Harricana–Lake McConnell glaciofluvial complex may extend discontinuously from a chain of islands in James Bay (Low, 1888; Wilson, 1938; Hardy, 1976, 1977) to the vicinity of Lake Simcoe, southern Ontario (Veillette, 1986; Figs. 1, 2), a distance of almost 1000 km! An interlobate origin for this complex has been proposed based on: (i) the trends of cross-cutting striae (Fig. 2), grooves (s-forms?) and crag-and-tails (Wilson, 1938; Tremblay, 1950; Hardy, 1976; Veillette, 1983, 1986, 1988, 1989, 1990; Veillette et al., 1989); (ii) the dispersion of indicator lithologies in tills (Veillette, 1986; Veillette et al., 1989); (iii) the orientations of eskers and moraines (Veillette, 1986; Veillette et al., 1989) (Fig. 1); and (iv) the distribution of C^{14} dates from organic sediment in lacustrine and pond sequences (Veillette, 1983, 1988, 1990; Richard et al., 1989). Hardy (1976) and Veillette (1986) suggested that the northern portion of the feature, the Harricana glaciofluvial complex (Fig. 1), was deposited time-transgressively between about 11.0 and 8.5 ka BP (the latter date marking the start of the proposed Cochrane events).

However, part of the Harricana glaciofluvial complex may be an esker (Allard, 1974; Trem-

Fig. 1. Pattern of eskers and moraines adjacent to the Harricana glaciofluvial complex mapped within the boxed area only, with the exception of the Sakami Moraine. Proposed extensions of the Harricana–Lake McConnell complex (Hardy, 1976; Veillette, 1986) indicated by large dots. The proposed northern island chain part of the Harricana complex (Wilson, 1938) extends north of the mapped area. Data sources: (1) relief simplified from Yelle (1976); (2) eskers mapped from Tremblay (1974), Chauvin (1977), Veillette (1986, 1990), Sado and Carswell (1987); (3) moraines mapped from Hardy (1976), Veillette (1986), Sado and Carswell (1987) and Vincent (1989).

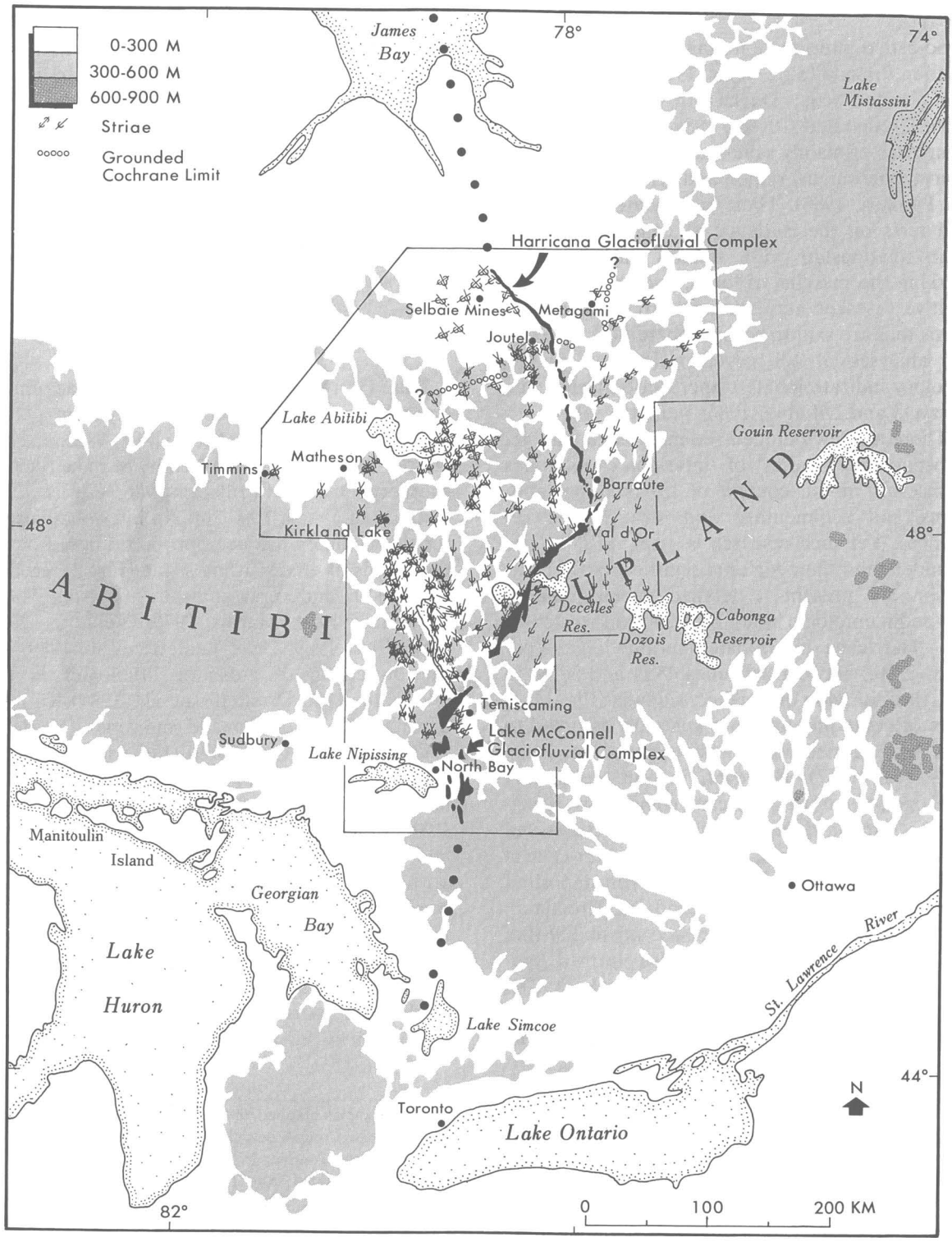
0-300 M
300-600 M
600-900 M
Striae
Grounded Cochrane Limit
James Bay
78°
74°
Lake Mistassini
Harricana Glaciofluvial Complex
Selbaie Mines
Metagami
Joutel
Lake Abitibi
Gouin Reservoir
Timmins
Matheson
Barraute
48°
Kirkland Lake
Val d'Or
ABITIBI
UPLAND
Decelles Res.
Dozois Res.
Cabonga Reservoir
Temiscaming
Lake McConnell Glaciofluvial Complex
Sudbury
Lake Nipissing
North Bay
Manitoulin Island
Georgian Bay
Lake Huron
Ottawa
St. Lawrence River
Lake Simcoe
44°
N
Toronto
Lake Ontario
82°
0
100
200 KM

blay, 1974; Hardy, 1976; Chauvin, 1977; Veillette, 1983, 1986, 1990). Indeed, Veillette (1990) described the section south of latitude 48°N as "un méga-esker en position interlobaire" (p. 86). Allard (1974) proposed that the complex is a series of time-transgressive subglacial esker segments, with superimposed subaqueous fans and punctuating deltas, between latitude 50°N and Lake Obalski (latitude 48°45′N, Fig. 3). He suggested that broader segments south of Lake Obalski to latitude 48°N record a transition to supraglacial and subaerial sedimentation.

In light of this previous research, if we are to understand its genesis and implications for ice-sheet dynamics, we need to know whether the Harricana glaciofluvial complex was formed (i) synchronously in a continuous conduit, or (ii) time-transgressively in a northwards migrating reentrant. Accordingly, we begin by comparing expected morphologies and sedimentary characteristics for these two cases (Table 1).

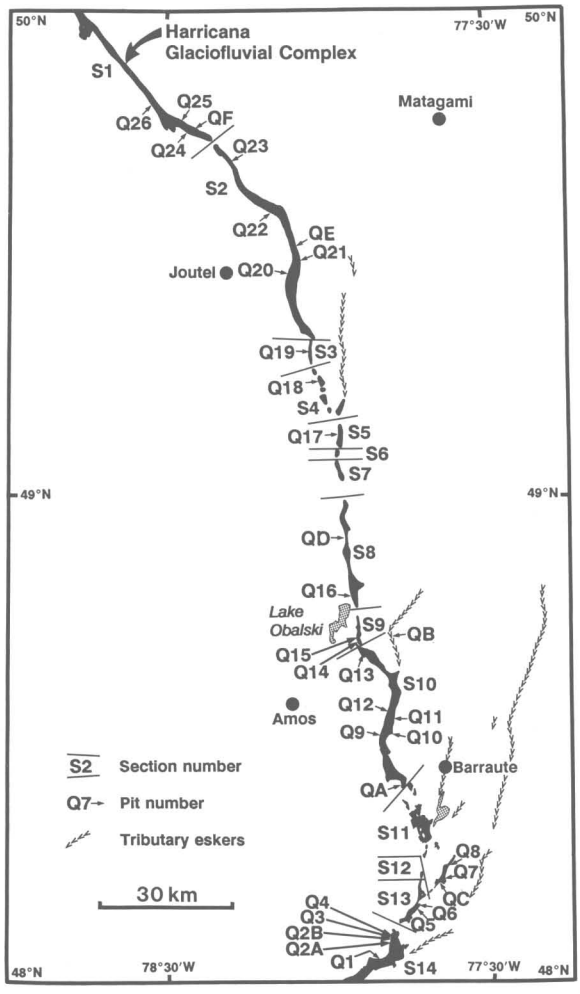

Fig. 3. Harricana glaciofluvial complex divided into depositional segments separated by "gaps". Location of pits, eastern tributary eskers, and Lake Obalski.

3. Geomorphology of the complex, clast characteristics and paleoflow direction estimates

North to south changes in geomorphology, clast lithology and roundness, and paleoflow direction estimates reflect the sedimentary environment and the glaciological conditions under which the complex formed. These, in turn, provide the context for more detailed sedimentary interpretations.

3.1. Geomorphology

The undulating crest-line of the Harricana glaciofluvial complex, constructed from 1:250,000 scale NTS maps, rises southwards from James Bay to latitude 48°N (Fig. 4). Air photographs show fourteen distinct segments between latitudes 48°N and 50°N (Figs. 3, 4; Brennand, 1993, p. 160). Segment lengths range from about 2 km to over 50 km, intervening gaps are between about 0.2 km and 4.5 km long. Most gaps are mantled by glaciolacustrine sediment and more recent organic material (Chauvin, 1977). Some expose bedrock, whereas others are occupied by rivers or lakes.

North of latitude 49°N (segments 1–7, Fig. 3) the complex is a single undulating ridge. It is

Fig. 2. Cross-striated sites mapped in dissected zone of Abitibi Uplands, and adjacent to the Harricana glaciofluvial complex (boxed area). Data sources: (1) relief simplified from Yelle (1976); (2) striae transferred from Veillette (1986); (3) proposed grounded Cochrane limit mapped from Veillette et al. (1991).

generally higher there than elsewhere, rising up to 60 m above the surrounding Cochrane terrain and Lake Ojibway clay plain. The ridge varies considerably in width: narrow parts have rounded crests and steep (15°–30°) side slopes; wide sections have broader, flatter crests and gentler (3°–10°) side slopes.

In the south (segments 8–14, Fig. 3) the complex is generally wider (up to 3.5 km), but widths vary. Some wide sections are low, standing less than 10 m above the surrounding Lake Ojibway clay plain. Others are steep-sided (> 15°) and more than 50 m high. Lateral and superimposed fans rarely punctuate depositional segments. Shorelines and spits record wave reworking during the Angliers and Early Kinojévis phases of Glacial Lake Ojibway (Fig. 4; Vincent and Hardy, 1979). South of latitude 48°N, the width of the complex increases locally to 10 km (cf. Veillette, 1986, 1990).

Elevated and linear glaciofluvial deposits imply deposition of the Harricana complex in an

Table 1
Expected characteristics [1] of linear synchronous and time-transgressive glaciofluvial deposits

	Synchronous deposition in a subglacial conduit	Time-transgressive deposition in a reentrant into the ice front
Geomorphology	Relatively linear ridges which may include "gaps" resulting from postdepositional erosion or nondeposition in a continuous conduit Depositional segments not punctuated by deltas or fans although lateral fans may occur Broadening of the deposit towards its downflow end Upslope, level or downslope path	Discrete depositional ridges punctuated by deltas or fans; typically beaded morphologic expression Downslope or level path
Down-complex trends in clast characteristics	**Lithology**: Trends depend upon the sediment source, and may be complicated by a mixture of lateral and local addition of sediment to the system	
	Roundness: *Relatively narrow conduit (upflow)*: Long transport distances and vigorous flows (particularly in a closed conduit) produce high sediment transport rates and low sedimentation rates, such that a mixture of well-rounded (long transport distance) and poorly-rounded (very angular to subrounded; local and laterally derived) clasts are favoured *Broad conduit (downflow)*: Under thinner ice the rate of conduit closure would decrease and the melting rate would adjust accordingly by decreasing flow velocity as the conduit became wider. Also, near a grounding line changes in subglacial water pressure cause local opening and closure of cavities adjacent to conduits. Both circumstances favour lower flow velocities, higher sedimentation rates and poorer clast rounding (a dominance of subrounded clasts).	There should be no gross clast roundness trends down the length of the complex. Rather, each segment should show upflow zones with poor rounding, and the proportion of rounded clasts should increase down-segment. Unless the segments are very long or there are numerous phases of fluvial reworking in a short segment (both of which are unlikely), a time-transgressive complex is unlikely to exhibit well-rounded clasts. In addition, a reentrant environment is at atmospheric pressure, favouring less vigorous flows and poorer clast rounding.
Paleoflow direction estimates	Relatively low variability in paleoflow direction estimates, although variability should increase at lateral fans built into subglacial cavities	Relatively high variability in paleoflow direction estimates where segments terminate in ice-marginal fans or deltas
Sedimentology	Minimal postformational disturbance, especially in the central section of the complex, although diapiric intrusion may exist Coarse gravel macroforms along the length of the complex Sand may alternate with gravel facies in vertical section at any location along the complex Sand and silt deposits increase in thickness and frequency downflow, and particularly in proximity to the ice margin or grounding line, where characteristic sedimentological associations related to decelerating flow on entry into a standing-water body may be observed.	Assuming a relatively static ice margin during deposition within a reentrant, the contact between gravel (proximal) and sand (more distal) units should be interfingered in vertical section. The distal ends of each segment should exhibit characteristic sedimentological associations related to decelerating flow on entry into a standing-water body. The nature of the associations will differ as a function of: height of water input, salinity of water body, and sediment concentration of the input.

[1] Derived from Banerjee and McDonald (1975), Gorrell and Shaw (1991), and Brennand (1994).

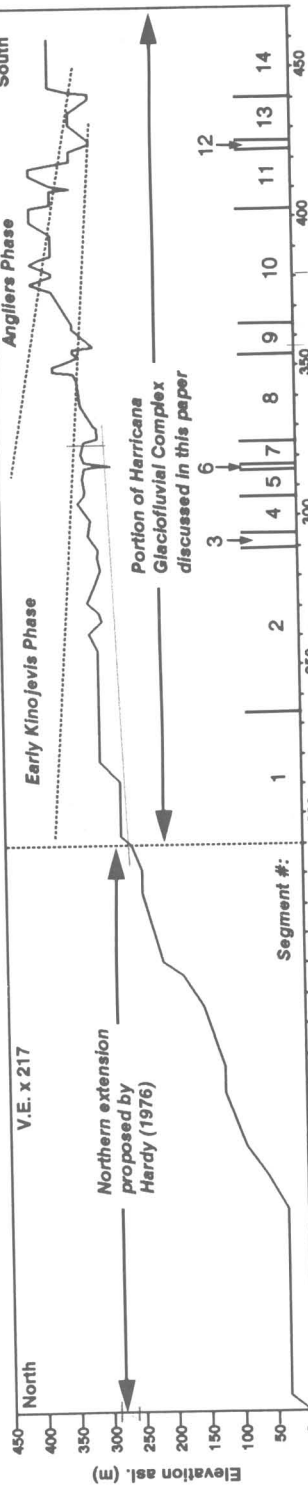

Fig. 4. Crest long profile along the axis of the Harricana glaciofluvial complex from Point de la Fougère Rouge on the coast of James Bay (51°48′54″N 79°21′18″W) to just south of Val d'Or (48°00′00″N 77°56′30″W), constructed from contours and spot heights on 1:250,000 scale NTS sheets. High-water levels of Angliers and Early Kinojévis phases (Vincent and Hardy, 1979) of Glacial Lake Ojibway indicate the approximate extent of littoral reworking of the Harricana complex.

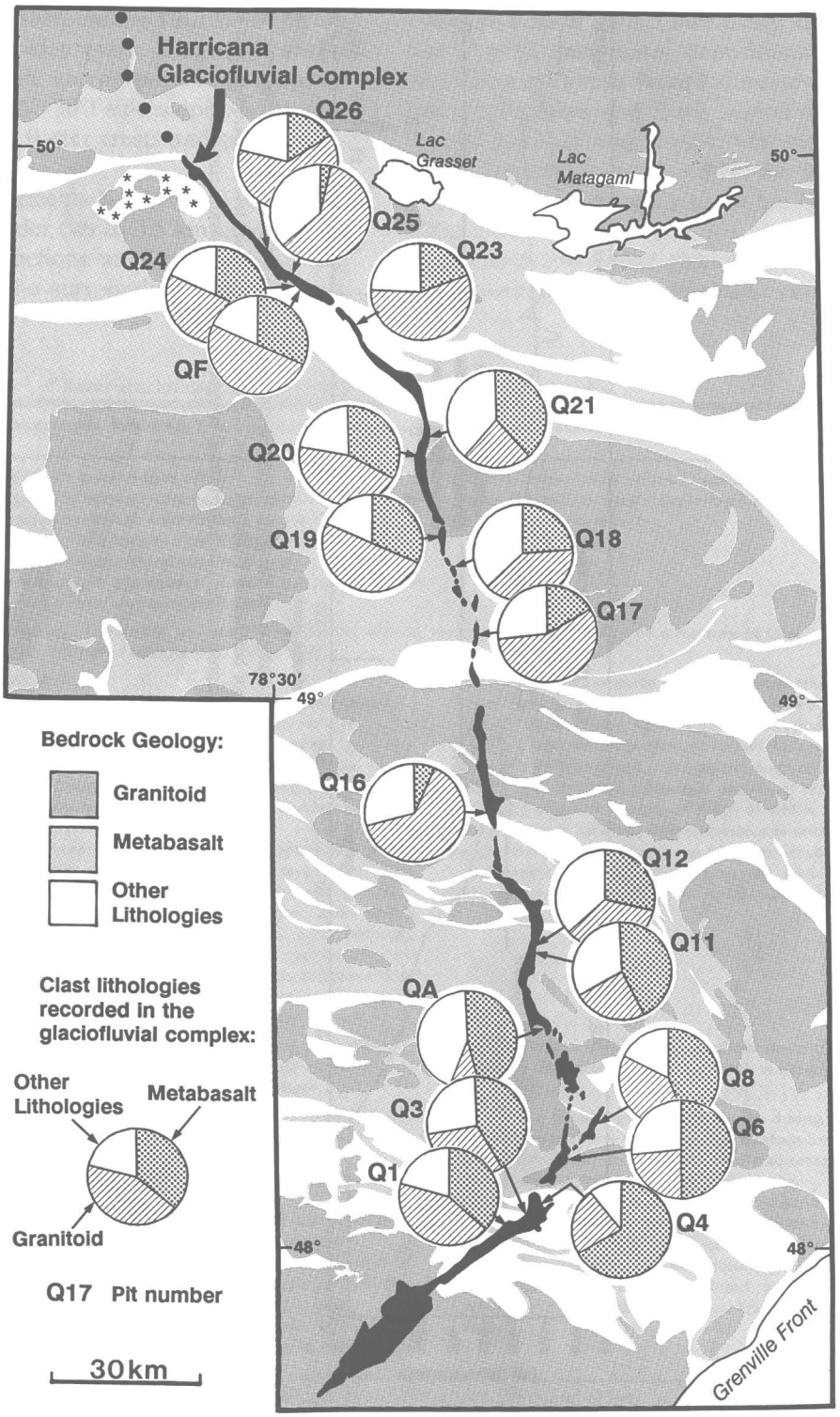
Harricana
Glaciofluvial Complex
Q26
Q25
Q24
Q23
QF
Q21
Q20
Q19
Q18
Q17
Q16
Q12
Q11
QA
Q8
Q3
Q6
Q1
Q4
Lac
Grasset
Lac
Matagami
50°
78°30′
49°
48°
Grenville Front
Bedrock Geology:
Granitoid
Metabasalt
Other
Lithologies
Clast lithologies
recorded in the
glaciofluvial complex:
Other
Lithologies
Metabasalt
Granitoid
Q17 Pit number
30km

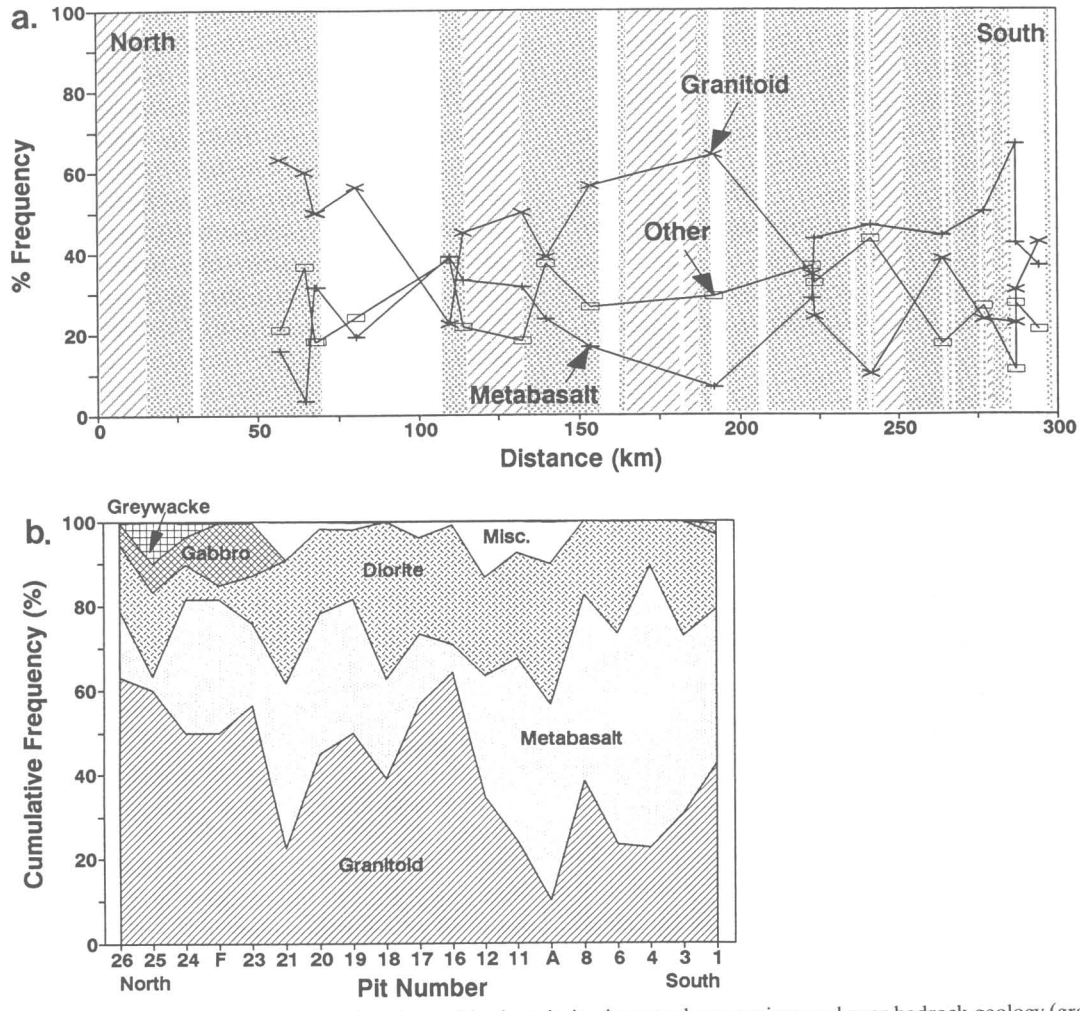

Fig. 6. (a) Percent frequency of granitoid and metabasaltic clasts in in-situ samples superimposed over bedrock geology (granitoid is diagonal shading, metabasaltic is stipple shading, other is unshaded) along the axis of the Harricana glaciofluvial complex. Geologic transect starts at 51°15′N 79°00′W and ends at 48°01′N 77°06′W. (b) Cumulative frequency of lithologies recorded in each pit (prefixed with "Q" in text) presented in downflow order. Lines connecting points are not meant to imply continuous variation, but merely to aid visual interpretation. Data summary in Brennand (1993).

ice-contact environment (e.g., Veillette, 1986). Gaps in such depositional landforms may result from periods of non-deposition in a time-transgressive system (cf. De Geer, 1897), from post-depositional erosion (e.g., by streams), or from non-deposition in constricted parts of a conduit (Brennand, 1994). It is by no means certain that all morphological gaps represent sedimentary dis-

Fig. 5. Proportion of clast lithologies from in-situ samples recorded in the Harricana glaciofluvial complex presented as pie graphs (data summary in Brennand, 1993) and superimposed over adjacent Abitibi Subprovince (Superior Province) bedrock geology (modified from MERQ-OGS, 1983). Stars show location of the gabbroic bedrock discussed in the text.

continuities; parts of the complex may be buried by Glacial Lake Ojibway or Tyrrell Sea sediments (Allard, 1974; Hardy, 1976).

3.2. Down-complex trends in in-situ clast characteristics

Gravel samples for clast lithology and roundness ranged from 30 to 294 in-situ clasts from fresh, vertical faces in commercial gravel pits. Clast size ranged from pebbles to small boulders, with cobbles predominant. Planimetric distance of samples is measured along the axis of the complex from the shore of James Bay (51°15′N 79°00′W). We limit this discussion to trends in the most abundant lithologic classes: granitoid and metabasaltic (Brennand, 1993, presents a full data summary). Very few metasedimentary clasts are preserved (Brennand, 1993); presumably clasts of these relatively soft lithologies were comminuted quickly (J.J. Veillette, pers. commun., 1993). The following description of the regional bedrock

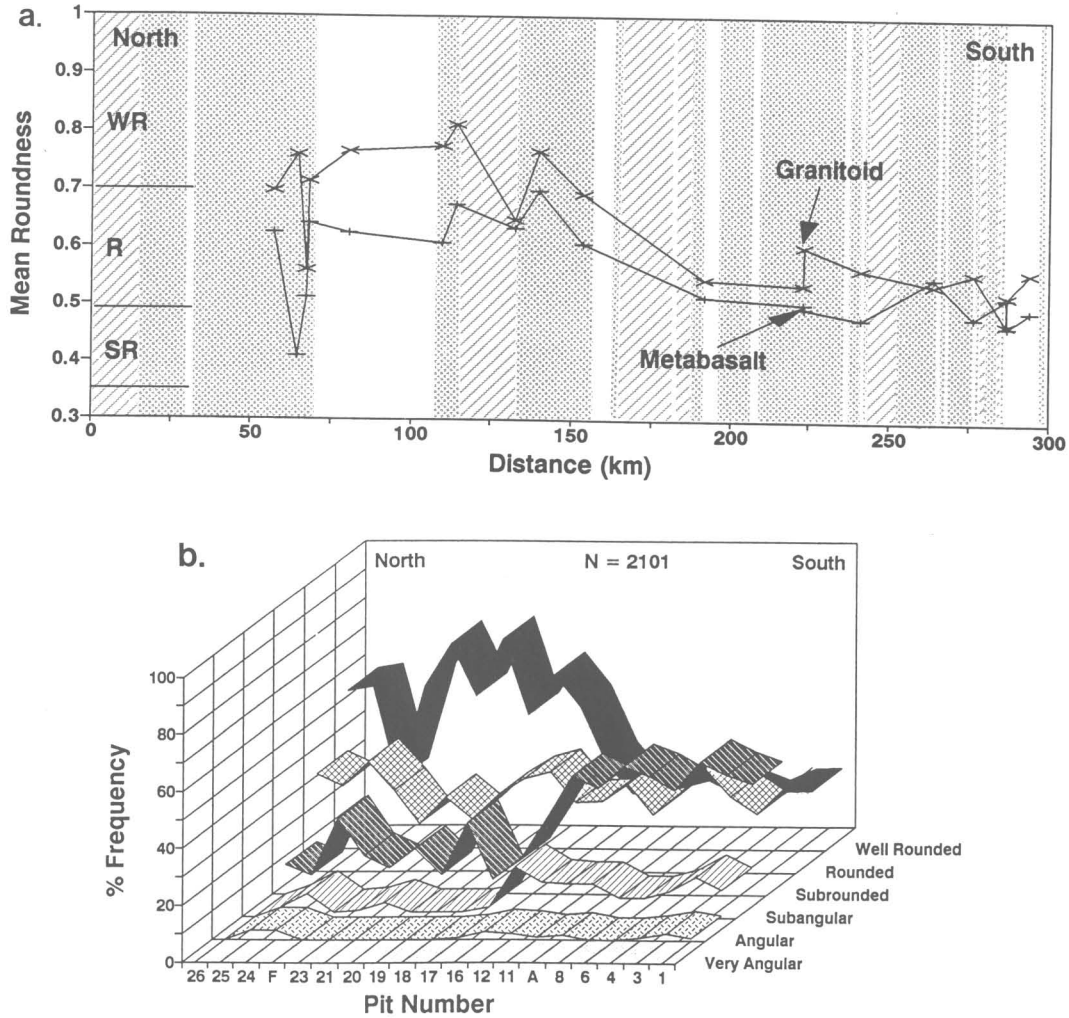

Fig. 7. (a) Downflow trend in the mean roundness (Powers, 1953) of granitoid and metabasaltic clasts in in-situ samples; geologic transect same as Fig. 6. *WR* is well rounded, *R* is rounded, *SR* is subrounded. (b) Frequency of occurrence of each visual roundness class by pit. Pits (prefixed with "Q" in text) arranged in downflow order. Lines connecting points are not meant to imply continuous variation, but merely to aid visual interpretation. Data summary in Brennand (1993).

geology provides background for interpreting down-complex trends.

Bedrock geology of the study area

The Harricana glaciofluvial complex crosses the Abitibi greenstone belt of the Precambrian (Neoarchean) Superior Province (MERQ-OGS, 1983). This belt of regionally deformed and metamorphosed volcanic and sedimentary rocks (e.g., basalts, gabbros, andesites, gneisses) also includes granitoid intrusions in discrete batholiths (Fig. 5) and numerous younger Precambrian diabase dikes. Precambrian (Neoarchean) metasedimentary (gneisses, wackes, siltstones) and granitoid rocks of the Opatica Subprovince lie north of the Abitibi Subprovince, with Paleozoic (Silurian) sedimentary rocks (carbonates, sandstones, shales and conglomerates) further to the north in the James Bay Lowlands.

Clast lithology

Metabasaltic and granitoid clasts are dominant in the Harricana complex gravel. To the north (north of pit Q11, ~225 km, Figs. 5, 6), granitoid clasts are most frequent in 11 out of 12 pits. By contrast metabasaltic clasts are most frequent in six out of seven pits to the south. These regional trends cannot be tied directly to bedrock distribution; metabasalt is widespread where granitoid clasts dominate to the north, and the very highest frequencies of granitoid clasts in the most northern pits do not seem to be associated with local granitoid bedrock (Figs. 5, 6). In addition, gabbroic clasts are unexpected because gabbro is only found some distance to the side of the complex (Figs. 5, 6b). Their presence implies lateral transport of sediment to the complex.

The lack of direct correspondence between clast frequency and local bedrock suggests that available geological maps may lack the necessary detail (J.J. Veillette, pers. commun., 1993), that lithologic characteristics were inherited from previously transported sediment not local bedrock, or that distance from bedrock source may not be the most important control on lithologic frequency. For example, where there was a combination of low deposition rates and vigorous clast transport, resistant clasts are expected to predominate; less resistant clasts would be quickly reduced to sand or finer sizes (Shaw and Kellerhals, 1982). Both vigorous transport and long transport distances may explain the preponderance of resistant granitoid clasts in the northern parts of the complex. By contrast, if flow had been less powerful and depositional rates had been high, differential comminution would have

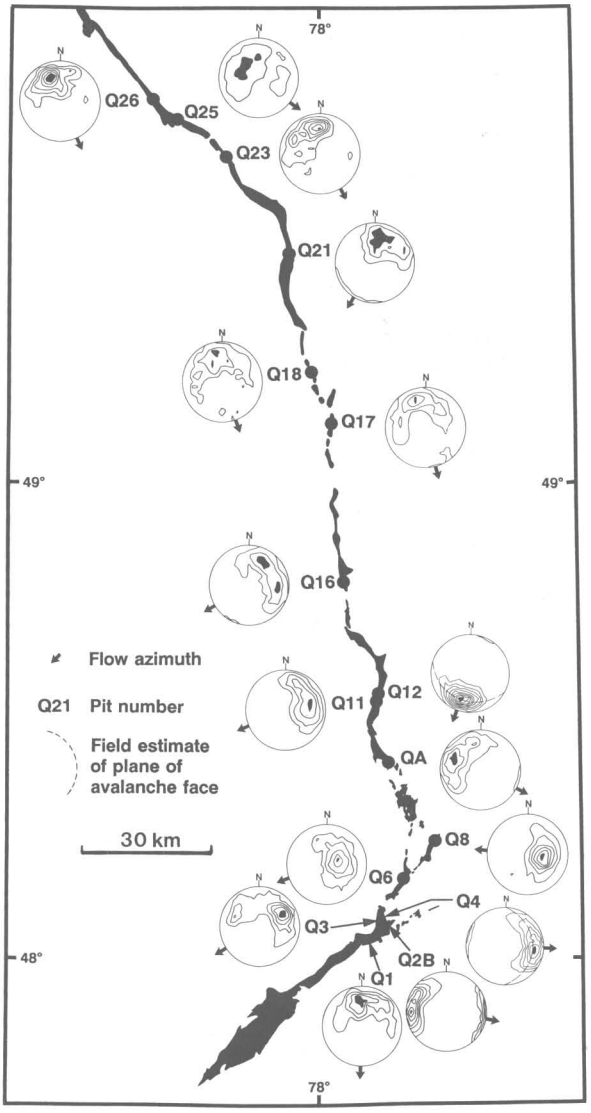

Fig. 8. Paleoflow direction estimates from gravel fabric measurements. Fabrics displayed as equal-area, lower-hemisphere projections. Statistics presented in Table 2.

been less pronounced: resistant and non-resistant lithologies would appear in proportions more closely reflecting their relative proportions in the source rocks. The relatively high proportions of less resistant metabasaltic clasts in the southern sections of the complex (Figs. 5, 6) may well indicate such reduced stream power relative to northern flow conditions.

These conclusions have implications for other clast properties, especially roundness. Clasts transported long distances by vigorous flows are expected to be rounder and to have comminuted faster than those transported short distances by less vigorous flows. Thus, vigour of transport may be as important as distance from source in determining roundness and lithological frequencies.

Clast roundness

Clast roundness was determined visually in the field (Powers, 1953) and each clast was assigned a value equal to the geometric mean of its visual roundness class. Clast roundness, generally sub- to well-rounded (Fig. 7), is consistent with fluvial transport (Sneed and Folk, 1958). More important in terms of our hypotheses, granitoid clasts are well rounded to rounded north of pit Q17 (~ 154 km, Fig. 7a) and rounded to subrounded south of pit Q12 (~ 223 km, Fig. 7a). The metabasaltic clasts show a similar trend (Fig. 7a). This trend is strikingly depicted in Fig. 7b where well-rounded clasts are predominant in the northern samples and sub-rounded is the modal class to the south.

Table 2
Bulk gravel fabric statistics

Pit #	Gravel Facies & macroforms	Sample Number	Flow Azimuth	Mean Dip	Vector Strength (S_1)	Significance Level[1]
Q1	Plane-bedded gravel	120	183°	44°	0.5870	99.0%
Q2B	Imbricate, polymodal fine gravel	60	100°	16°	0.7762	99.0%
Q3	Alternating oblique accretion avalanche bed macroform ('flipped' clasts[2] from both east and west sets)	120	238°	41°	0.5477	99.0%
Q4	Oblique accretion avalanche bed macroform; east side of complex ('parallel' clasts[3])	42	(271°) 91°	28°	0.7431	99.0%
Q6	Bimodal, massive, clast-supported gravel from large, downflow-dipping, rhythmically-graded beds ('flipped' clasts)	60	250°	67°	0.6465	99.0%
Q8	East side of pseudoanticlinal macroform	60	275°	56°	0.7031	99.0%
QA	Heterogeneous, unstratified gravel	60	115°	37°	0.6397	99.0%
Q11	Imbricate, polymodal, matrix-rich gravel	60	246°	41°	0.6485	99.0%
Q12	Large cross-bedded gravel or south-dipping avalanche beds of macroform ('parallel' clasts[3])	97	(8°) 188°	33°	0.8158	99.0%
Q16	Heterogeneous, unstratified gravel	60	240°	38°	0.5573	99.0%
Q17	Bimodal, massive, clast-supported gravel from large-scale, downflow-dipping, rhythmically-graded beds ('flipped' clasts)	60	163°	36°	0.5318	99.0%
Q18	Heterogeneous, unstratified gravel	149	161°	41°	0.5176	99.0%
Q21	Imbricate gravel lag	63	181°	37°	0.5663	99.0%
Q23	Upflow-inclined, plane-bedded gravel	160	149°	39°	0.5848	99.0%
Q25	Bimodal, massive, clast-supported gravel from exposure-scale, downflow-dipping, rhythmically-graded beds ('flipped' clasts)	30	126°	59°	0.4870	99.0%
Q26	Heterogeneous, unstratified gravel; imbricate, polymodal, matrix-rich coarse gravel	170	157°	42°	0.7001	99.0%

[1] Significance level of sample being non-random, according to test statistic (S_1/S_3) of Woodcock and Naylor (1983).
[2] Clast *ab*-planes dip upflow with respect to the field-estimated avalanche face.
[3] Clast *ab*-planes dip downflow and are approximately parallel to the field-estimated avalanche face. Flow azimuth (no brackets) assumed to be 180° to azimuth if imbrication inferred (brackets).

We conclude from the roundness analysis that transport distances and vigour of transport were probably greater in the northern part of the complex than in the southern. Lithological analysis gave the same conclusion. The north to south changes in roundness and lithology coincide with gross change in the geomorphology of the complex.

3.3. Paleoflow direction estimates

Paleoflow direction measurements were recorded from gravel fabrics (clast *ab*-planes) and cross-bedded and cross-laminated sand along the length of the Harricana complex (Tables 2, 3; Figs. 8, 9). Mean paleoflow azimuths for a site were determined from numerous measurements on gravel clasts or sand structures throughout a pit (30 to 170 clasts and 5 to 110 cross-bedded and cross-laminated sets per pit); they are only rarely based on measurements from a single unit within a pit. All flow azimuths are unidirectional and statistically significant at the 99% confidence level.

If gravel fabrics are related to the flow dynamics causing gravel facies and macroforms (Brennand, 1994), paleoflow estimates from them are unidirectional towards the south. Estimates from cross-bedded and cross-laminated sand show a similar trend but with greater variability in the south. Such paleoflow directions favour deposition in an ice-walled channel, either a subglacial conduit (cf. Brennand, 1994) or tightly constrained reentrant (cf. Cheel, 1982), perhaps widening to the south.

3.4. Environmental constraints inferred from geomorphology, clast characteristics, and paleoflow direction estimates

The Harricana complex is an elevated and relatively continuous glaciofluvial deposit, rising and widening downflow towards an ice margin or grounding line. For meltwater to have flowed uphill for several hundred kilometres, it must have been under hydrostatic pressure in a subglacial, closed conduit (cf. Shreve, 1972).

The relatively high and narrow ridge and low variability of paleoflow direction in the northern

Table 3
Paleoflow direction statistics derived from cross-bed and cross-lamination measurements

Pit Number	Sample Number (n)	Vector Mean (θ)	Mean Resultant Magnitude (R)[1]	Standard Error (S_θ)	Approximate deviation of R from the axis of the complex
Q1	80	257°	0.9138	2.7700°	17°
Q2A	6	177°	0.9979	3.3035°	7°
Q2B[2]	18	219°	0.9596	3.8585°	49°
Q3	65	187°	0.9057	3.0868°	7°
Q4[2]	15	189°	0.9917	2.0958°	19°
Q5	5	211°	0.9767	5.1594°	9°
Q8	5	253°	0.9622	7.3109°	48°
Q11	34	176°	0.8422	5.7404°	24°
Q12	10	222°	0.9876	2.5721°	22°
Q16[2,3]	65	191°	0.8059	4.5703°	31°
Q17	110	166°	0.9299	2.0789°	1°
Q20	31	204°	0.9561	2.9455°	19°
Q21	45	200°	0.8579	4.6631°	10°

[1] All samples show a preferred trend at $\alpha = 0.01$. Significance level (α) determined from critical values of R for Rayleigh's test for the presence of a preferred trend (Curray, 1956; Davis, 1986).
[2] From subaqueous fans or grounding-line deposits.
[3] Incudes measurements on some regressive ripples in the lee of a dune.

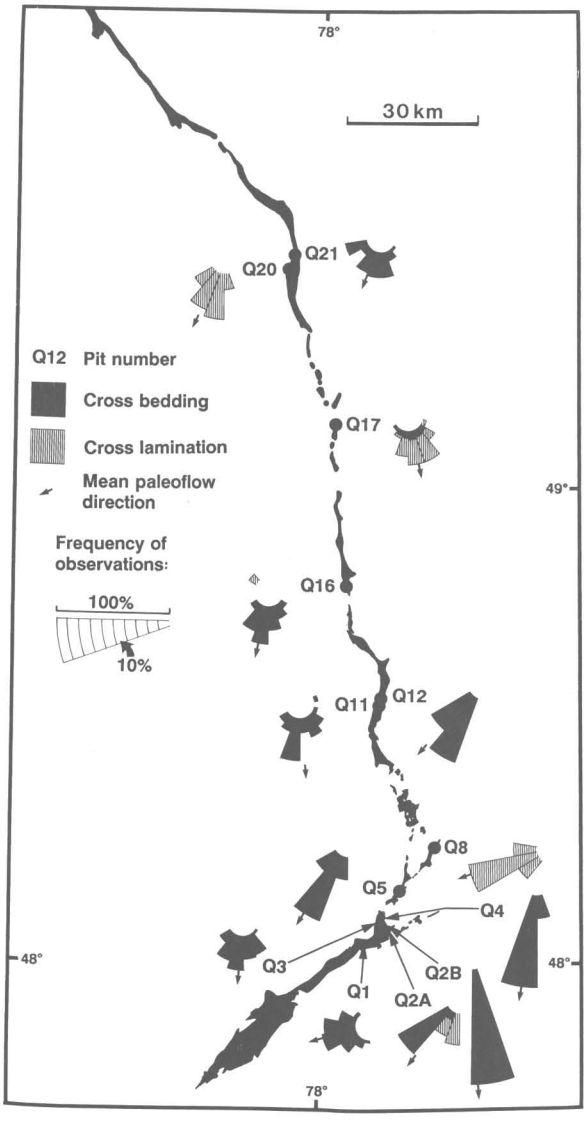

Fig. 9. Paleoflow direction estimates from cross-bed and cross-lamination measurements in sand. Statistics presented in Table 3.

part of the Harricana complex suggest a relatively narrow conduit there. As well, the high clast roundness values and poorer preservation of less resistant clasts suggest vigorous transport and high flow power to the north. The combination of a narrow conduit and high flow power requires a high conduit closure rate by ice flow (Röthlisberger, 1972); inflowing ice replaces that ablated by frictional heat generated by the flow. Together with stream power, the most important control on closure rate would have been ice thickness (h); closure rate increases with $(p_i - p_w)^m$, where p_i is ice overburden pressure ρgh, p_w is conduit water pressure, m is a constant > 1, ρ is ice density, and g is acceleration due to gravity (Paterson, 1981). With these controls in mind, it is clear that the relatively narrow and uniform widths of the northern part of the complex indicate that, despite increasing discharge downflow, the closure rate resulting from ice thickness was sufficiently high to maintain a narrow conduit and sufficiently uniform to maintain fairly constant width over a long distance. Under these conditions, if ice thickness had decreased appreciably, conduit width would have increased accordingly.

By contrast, the southern part of the complex is generally wider and exhibits greater paleoflow direction variability than the northern part. This widening is best explained if the ice sheet was appreciably thinner to the south, unless discharge increased dramatically. Naturally, thinning is to be expected as the margin of an ice sheet is approached. Thus, widening to the south probably indicates that the closure rate decreased towards the ice margin and the melting rate adjusted accordingly with decreasing velocity as the conduit enlarged. Transport distances were probably shorter. Less vigorous flows and higher depositional rates favoured better preservation of less resistant clasts in the south.

The contrasts in transport regime deduced from clast characteristics make sense if the northern and southern parts were formed subglacially and synchronously in a continuous conduit; transport regime related to changing conditions with distance from the grounding line. In this synchronous, subglacial depositional model, gaps may have originated as nondepositional zones within the continuous conduit (Shreve, 1985), or were eroded after formation of a continuous sedimentary complex.

The expected geomorphic, paleoflow direction and clast characteristics for the alternative, time-transgressive recessional model (Table 1) are not observed. If each segment of the complex records deposition over a discrete time period and the

Table 4
Gravel facies deposited under closed-conduit and open-channel conditions

Facies	Structural characteristics[1]	Main sediment support mechanisms	Origin of structure	Interpretation	
				Closed conduit[3]	Open channel
Heterogeneous, unstratified gravel	Vaguely lenticular, textural organization of heterogeneous gravel; ungraded; framework supported; cluster imbrication with a(t) b(i) and a(p) a(i) and high dips; tabular or pseudoanticlinal bed geometry	Fluid turbulence; bed	Longitudinal sediment sorting during tractional transport; sorting associated with the development of cluster bedforms	Facies within a composite or pseudoanticlinal macroform; deposition during the waning stages of floods	(i) Expansion bar[4]; (ii) Waning flood-flow deposit[5]
Massive, imbricate, clast-supported gravel[2]	Massive; relatively bimodal and clast-supported; generally ungraded; pervasive imbrication with a(t) b(i) and a(p) a(i) and high dips; tabular or pseudoanticlinal bed geometry	Fluid turbulence; bed	Deposition primarily from traction transport with minor suspension and saltation transport	Facies within a composite or pseudoanticlinal macroform	(i) Longitudinal bar[4, 6]
Plane-bedded gravel	Plane bedded, becoming more massive in coarser units; polymodal, graded or longitudinally sorted beds; a(t) b(i) imbrication dominant; tabular bed geometry	Bed; fluid turbulence	Deposition primarily from traction transport	Facies within a composite macroform	(i) Longitudinal gravel bar (Expansion bar?)[4, 7]; (ii) Diffuse gravel sheets[8]
Imbricate, polymodal gravel	Texturally polymodal although some may be more matrix-rich; ungraded or weak normal or inverse-to-normal grading; a(p) a(i) and a(t) b(i) imbrication; tabular or lenticular bed geometry	Fluid turbulence; dispersive pressure; buoyancy; hindered settling	Deposition from highly concentrated dispersion (homogenous or heterogenous)	May form in-phase wave structures associated with the establishment of a density interface at points of flow expansion	(i) Hyperconcentrated flood-flow deposit[9]; (ii) Longitudinal bar with later infiltration[6]
Cross-bedded gravel	Graded foreset beds: (A) Base - bimodal, clast-supported gravel occasionally with convoluted laminae in sand (B) Middle - Openwork gravel (C) Upper - Openwork gravel (smaller grain size)	Fluid turbulence; bed	Bedform migration or macroform progradation; longitudinal sediment sorting during transport of heterogeneous gravel, and lee-side deposition of suspended load in return flow beneath a separation eddy	Large gravel dunes; facies within composite macroform, associated with bedform migration or macroform progradation	(i) Longitudinal gravel bar4, 7; (ii) Transverse bar[6]

[1] *a*(t) *b*(i): clast *a*-axis transverse to flow direction, *b*-axis imbricate; *a*(p) *a*(i): clast *a*-axis parallel to flow direction and imbricate.
[2] Not identified in the Harricana complex.
Interpretations derived from: [3] Brennand (1994); [4] Baker (1978); [5] Fraser and Bleuer (1988); [6] Ringrose (1982); [7] Rust (1984); [8] Smith (1990); [9] Smith (1986).

Table 5
Fabric and transport orientation data for gravel facies and structures

Unit Number	Sedimentary Facies/Structure	Sample Number	Flow Azimuth	Mean Dip of ab-plane	Vector Strength (S_1)	Significance Level [1]	Transport Orientation Data			
							a(t)	a(p)	Cobbles[2]	Pebbles[2]
QA/1-1	Heterogeneous, unstratified gravel	60	115°	37°	0.6397	99.0%	63.3%	31.7%	a(t)	[a(p)]
Q16/4-2	Heterogeneous, unstratified gravel	60	240°	38°	0.5573	99.0%	48.3%	50.0%	a(t)	a(p)
Q18/1-4	Heterogeneous, unstratified gravel	99	152°	42°	0.5329	99.0%	54.2%	42.4%	a(t)	[a(p)]
Q18/1-1	Heterogeneous, unstratified gravel	50	176°	36°	0.5051	99.0%	N/A	N/A	N/A	N/A
Q23/2-1	Heterogeneous, unstratified gravel	60	152°	38°	0.6507	99.0%	45.0%	48.3%	equal	[a(p)]
Q26/1-2	Heterogeneous, unstratified gravel	110	162°	44°	0.6795	99.0%	N/A	N/A	N/A	N/A
Q1/1-2RHS	Plane-bedded gravel	60	190°	45°	0.7013	99.0%	50.0%	43.3%	a(t)	equal
Q1/1-3LHS	Plane-bedded gravel	60	162°	41°	0.4888	99.0%	45.0%	53.3%	[a(t)]	a(p)
Q23/1-2	Inclined, plane-bedded gravel	160	149°	39°	0.5848	99.0%	56.8%	35.6%	a(t)	[a(p)]
Q2B/2-1	Imbricate, polymodal gravel with in-phase wave surfaces	60	100°	16°	0.7762	99.0%	N/A	N/A	N/A	N/A
Q11/1-1	Imbricate, polymodal, matrix-rich gravel with tabular geometry	60	246°	41°	0.6485	99.0%	48.3%	51.7%	[a(t)]	a(p)
Q26/1-1LHS	Imbricate, polymodal, matrix-rich gravel with poorly defined convex-up bedding surfaces	60	151°	38°	0.7496	99.0%	63.2%	34.2%	a(t)	none
Q23/1-1: Full sample	Large cross-bedded gravel	59	326°	2°	0.6016	99.0%	42.4%	49.2%	[a(p)]	a(p)
Q23/1-1: 'Parallel' clasts[3]	Large cross-bedded gravel	28	(328° 148°	29°	0.6986	99.0%	15.3%	27.1%	[a(p)]	a(p)
Q23/1-1: 'Flipped' clasts[4]	Large cross-bedded gravel	31	140°	23°	0.7445	99.0%	27.1%	22.0%	[a(t)]	[a(t)]
Q6/1-2: 'Flipped' clasts[4]	Bimodal, massive, clast-supported gravel from large-scale, downflow-dipping, rhythmically-graded, tabular beds	60	250°	67°	0.6465	99.0%	43.3%	53.3%	a(p)	[a(p)]
Q17/1-7RHS: 'Flipped' clasts[4]	Bimodal, massive, clast-supported gravel from large-scale, downflow-dipping, rhythmically-graded, tabular beds	60	163°	36°	0.5318	99.0%	38.3%	60.0%	a(p)	equal
Q25/1-1b: 'Flipped' clasts[4]	Bimodal, massive, clast-supported gravel from large-scale, downflow-dipping, rhythmically-graded, tabular beds	30	126°	59°	0.4870	99.0%	36.7%	56.7%	a(p)	none
Q12/1-1aRHS (east): Full sample	Large cross-bedded gravel or south-dipping avalanche beds of composite macroform	60	29°	18°	0.5063	99.0%	45.0%	53.3%	equal	a(p)

Q12/1-1aRHS (east): 'Parallel' clasts[3]	Large cross-bedded gravel or south-dipping avalanche beds of composite macroform	35	(35°) 215°	29°	0.7752	99.0%	25.0%	33.3% [a(p)]	a(p)
Q12/1-1aRHS (east): 'Flipped' clasts[4]	Large cross-bedded gravel or south-dipping avalanche beds of composite macroform	25	205°	48°	0.5998	99.0%	20.0%	20.0% [a(t)]	[a(p)]
Q12/1-1aLHS (west): Full sample	Large cross-bedded gravel or south-dipping avalanche beds of composite macroform	60	8°	0.08°	0.6066	99.0%	45.0%	55.0% a(p)	equal
Q12/1-1aLHS (west): 'Parallel' clasts[3]	Large cross-bedded gravel or south-dipping avalanche beds of composite macroform	26	(6°) 186°	32°	0.8620	99.0%	16.7%	26.7% [a(p)]	a(p)
Q12/1-1aLHS (west): 'Flipped' clasts[4]	Large cross-bedded gravel or south-dipping avalanche beds of composite macroform	34	188°	29°	0.7424	99.0%	28.3%	28.3% a(p)	a(t)
Q12/1-1bLHS (west): Full sample	Large cross-bedded gravel or south-dipping avalanche beds of composite macroform	60	17°	19°	0.6959	99.0%	33.3%	63.3% equal	a(p)
Q12/1-1bLHS (west): 'Parallel' clasts[3]	Large cross-bedded gravel or south-dipping avalanche beds of composite macroform	36	(14°) 194°	36°	0.8824	99.0%	20.0%	38.3% equal	a(p)
Q12/1-1bLHS (west): 'Flipped' clasts[4]	Large cross-bedded gravel or south-dipping avalanche beds of composite macroform	24	202°	17°	0.7802	99.0%	13.3%	25.0% equal	a(p)
Q3/2-4LHS (East): 'Flipped' clasts[4]	Oblique-accretion, avalanche-bed macroform (east set of alternating sequence)	60	131°	36°	0.5783	99.0%	48.3%	48.3% [a(p)]	[a(t)]
Q3/2-4RHS (West): 'Flipped' clasts[4]	Oblique-accretion, avalanche-bed macroform (west set of alternating sequence)	60	241°	37°	0.7852	99.0%	60.0%	31.7% a(t)	none
Q4/3-3 (East): Full sample	Oblique-accretion, avalanche-bed macroform dipping to east	60	275°	18°	0.6145	99.0%	33.3%	66.7% a(p)	a(p)
Q4/3-3 (East): 'Parallel' clasts[3]	Oblique-accretion, avalanche-bed macroform dipping to east	42	(271°) 91°	28°	0.7431	99.0%	18.3%	51.7% a(p)	a(p)
Q4/3-3 (East): 'Flipped' clasts[4]	Oblique-accretion, avalanche-bed macroform dipping to east	18	99°	25°	0.5590	99.0%	15.0%	15.0% equal	equal
Q21/5-1LHS: Full sample	Oblique-accretion, avalanche-bed macroform dipping to south-southeast	60	339°	24°	0.5158	99.0%	48.3%	41.7% a(t)	[a(t)]
Q21/5-1LHS: 'Parallel' clasts[3]	Oblique-accretion, avalanche-bed macroform dipping to south-southeast	36	(344°) 164°	43°	0.7193	99.0%	31.7%	28.3% [a(t)]	equal
Q21/5-1LHS: 'Flipped' clasts[4]	Oblique accretion avalanche bed macroform dipping to south-southeast	24	140°	27°	0.7056	99.0%	16.7%	13.3% [a(t)]	equal
Q8/1-1LHS (east)	East side of pseudoanticlinal macroform	60	275°	56°	0.7031	99.0%	53.3%	43.3% [a(t)]	[a(p)]

N/A = no data available.

[1] Significance level of sample being non-random, according to test statistic (S_1 / S_3) of Woodcock and Naylor (1983).

[2] Dominant *a*-axis orientation for cobble and pebble grain sizes; [...] indicates $< 5\%$ difference in dominant orientation of *a*-axes.

[3] "Parallel"clasts: *ab*-planes dip downflow and are approximately parallel to field-estimated dip of avalanche face or foreset. Flow azimuth (no brackets) assumed to be 180° to azimuth if imbrication inferred (brackets).

[4] "Flipped" clasts: *ab*-planes dip upflow with respect to avalanche face or foreset.

intervening gaps represent intervals of nondeposition during retreat, then prominent subaqueous fans are to be expected at the distal ends of each segment. These were not always found. Furthermore, sediment deposited sequentially in a northwards migrating, broad, marginal conduit would have covered the narrow sedimentary ridge in the northern part. This was clearly not the case—clast

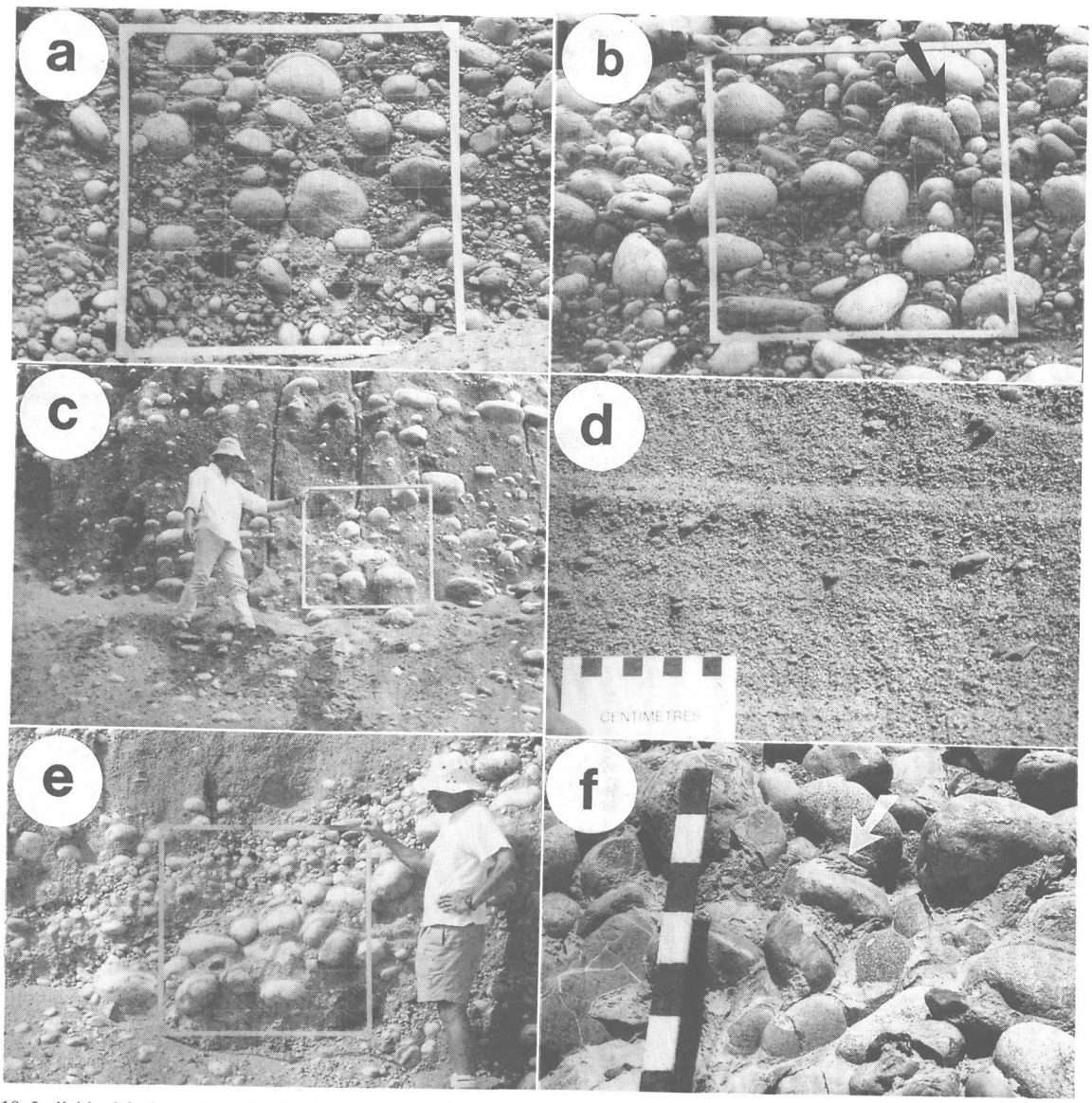

Fig. 10. Individual facies within the Harricana complex. (a) Heterogeneous, unstratified gravel exhibiting vaguely lenticular, textural organization (unit Q21/1-1aRHS). Grid is 1 m^2. (b) Heterogeneous, unstratified gravel with imbricate clast clusters (arrow). (c) Imbricate, polymodal, matrix-rich coarse gravel with clasts occurring preferentially along poorly defined convex-up bedding surfaces (unit Q26/1-1LHS, Table 5). (d) Imbricate, polymodal fine gravel with diffusely graded laminae (unit Q2B/2-1, Table 5). (e) Grading in cross-bedded gravel (unit Q23/1-1, Table 5). (f) Bimodal, clast-supported gravel with contorted laminae (arrow) in sand matrix at the base of large-scale, downflow-inclined, tabular beds. Scale 10-cm intervals.

characteristics and the landform itself are quite distinct in the northern and southern parts of the complex. Hence, we reject the time-transgressive, recessional model in favour of synchronous deposition of the Harricana complex in a continuous conduit, narrow and of relatively uniform width in the north and wider to the south. However, transgressive subaqueous fans and grounding-line deposits do form part of the Harricana complex in the south and are discussed later.

Gabbro clasts indicate lateral transport of sediment into the Harricana complex, delivered by way of tributary conduits or transported englacially or by local subglacial deformation. Lateral transport is a necessary consequence of the balance between melting of the conduit walls and replacement of ice by inflow. Sediment within the basal ice or deforming subglacially would have been transported along flowlines converging on the complex.

Now we describe and interpret the detailed sedimentology of the Harricana complex in view of the general environmental conditions for its deposition. Our aim is to gain an understanding from the sediment of the processes and subenvironments within such enormous conduits. Establishing subglacial conditions first, on evidence which is independent of detailed sedimentary sequences, is necessary in this case because many bedforms and their associated structures are common to both open channels and closed conduits (Table 4).

4. Sedimentology of the Harricana glaciofluvial complex

We apply an architectural approach (cf. Miall, 1985; Brennand, 1994) in a sedimentary study of 31 extensive exposures in commercial gravel pits. Grain size of exposed deposits was estimated or measured in the field. Primary sedimentary structures were described and recorded by photographs and sketches. Paleoflow directions were estimated (Figs. 8, 9; Tables 2, 3, 5). Gravel transport dynamics are inferred from a record of clast *a*-axis orientation with respect to flow azimuth (orientation of maximum dip of *ab*-planes) (Table 5).

4.1. Gravel facies and gravel–sand couplets

Gravel facies are the building blocks of the Harricana complex. Their interpretation acts as an essential aid to understanding larger-scale macroforms. Four gravel facies are identified: heterogeneous unstratified; plane-bedded; cross-bedded; and imbricate, polymodal. The latter shares characteristics with sandy in-phase wave structures. Vertically stacked, gravel–sand couplets are widespread in the Harricana complex.

Heterogeneous, unstratified gravel

Heterogeneous, unstratified gravel (Figs. 10a, 10b) is the most common facies in the Harricana complex. It is texturally polymodal, ranging from boulders to fine sand and silt; cobbles and boulders are predominant. Beds are 1–5 m thick with erosional lower contacts. Bed geometry may be tabular or pseudoanticlinal. This facies is mostly framework-supported (cf. Rust and Koster, 1984) and is not graded (Figs. 10a, 10b). Vaguely delineated lenses of polymodal, bimodal clast-supported, bimodal matrix-supported, and openwork gravel may all appear at random in the same bed (Fig. 10a; Brennand, 1994). Imbricate clusters of larger clasts are common, otherwise there is no apparent preferred clast orientation or dip (Fig. 10b). Although imbricate cobbles are generally oriented with their *a*-axis transverse to flow direction (*a*(t)), there is a significant proportion of *a*-axis parallel (*a*(p)) clasts, particularly pebbles (Table 5). Mean dip angles of clast *ab*-planes are generally steep (36°–44°, Table 5).

Deposition from turbulent, relatively low-viscosity flows is inferred for the heterogeneous, unstratified gravel facies. Whereas cobbles mainly rolled along the bed, pebbles moved by saltation and in suspension (cf. Rust, 1972; Johansson, 1976). Thus, sediment in transport was supported mainly by the bed and by turbulence. Steeply dipping clasts are attributed to the high frequency of clast-to-clast contacts during deposition of this framework-supported facies (Rust, 1972).

The vaguely lenticular organization in heterogeneous, unstratified gravel may have been caused by longitudinal sediment sorting (Iseya and Ikeda,

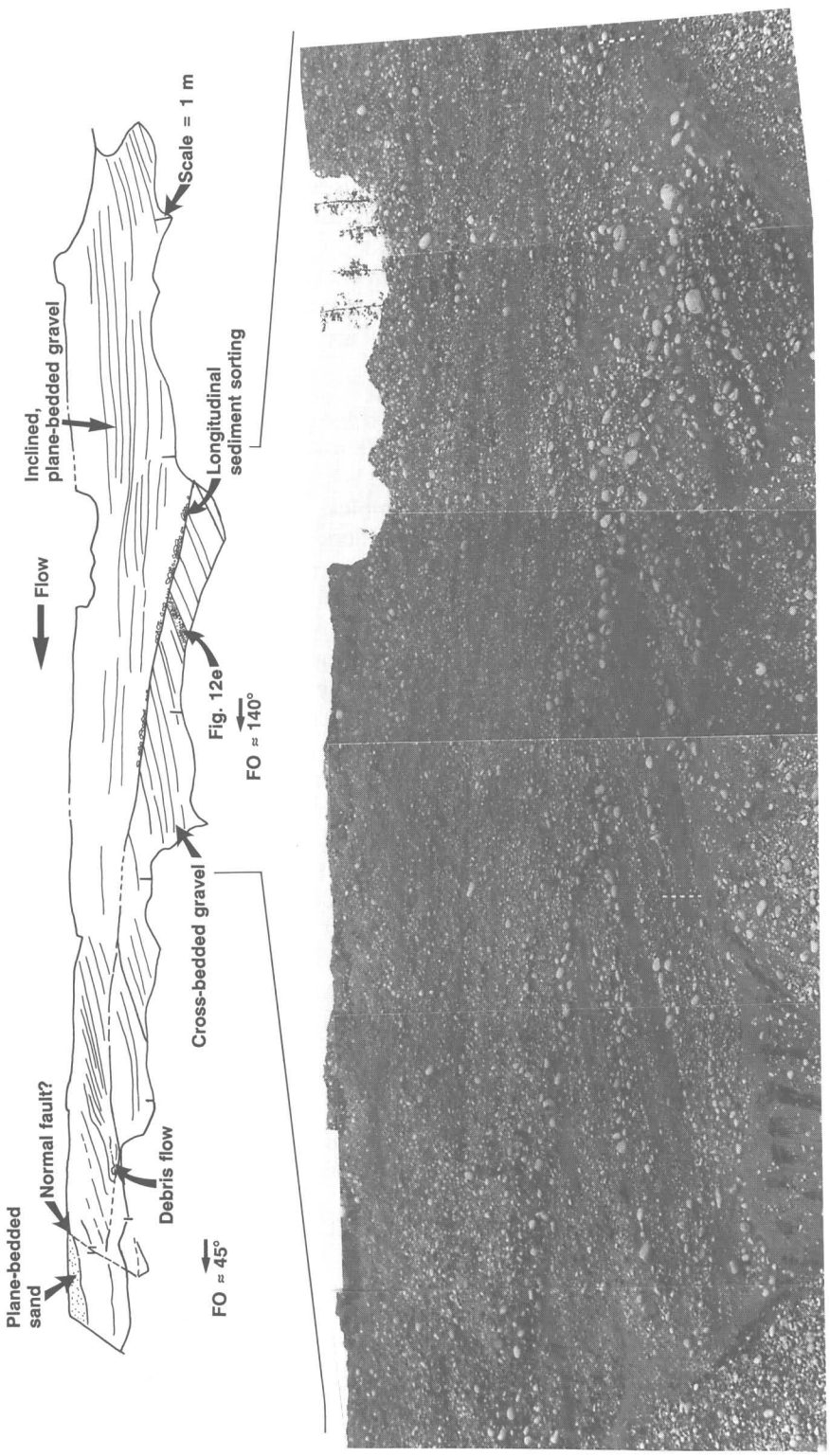

Fig. 11. Sediments exposed in long axis of part of a composite macroform exhibiting two superimposed dunes at pit Q23. Note, only a small portion of the sketched face is shown in the photograph. *FO* is approximate pit face orientation.

1987), resulting from larger clasts having higher transport velocities than smaller ones where bed shear stresses are well above critical for all sizes present (cf. Meland and Norrman, 1969). We can imagine preservation of this sorting under high rates of sedimentation in rapidly waning flow or at sudden flow expansions in conduits or to the lee of bedforms with slip faces. Some imbricate gravel clusters may record cluster bedforms, formed during the waning stages of floods (cf. Brayshaw, 1984).

The coarseness of this facies indicates deposition under high flow power; entrainment velocities of about 1.5–10.3 m s^{-1} are estimated for the largest clasts (-9ϕ) (Williams, 1983). These velocities are comparable to those reported for flood flows (jökulhlaups) resulting from the drainage of ice-dammed lakes (cf. Elfström, 1987).

Plane-bedded gravel

Plane-bedded, polymodal cobble and pebble gravel with granules and sand forms sets 2–6 m thick. Individual beds are usually close to horizontal, though some may be inclined upflow at low angles in tabular units (Fig. 11). They are 0.1–0.5 m thick. This facies is sorted in places with openwork, matrix-supported, clast-supported and polymodal lenses along bedding planes (Fig. 11). Imbricate clusters of larger clasts are common with mainly *a*(t) and dips of *ab*-planes comparable to those of the heterogeneous, unstratified gravel facies (Table 5). The *a*-axes of some pebbles are oriented parallel to flow (Table 5).

Stratification and imbrication in plane-bedded gravel are indicative of deposition from traction transport in low-viscosity flows. Some smaller clasts may have been transported in turbulent suspension or saltation. Plane beds may result from downflow migration of low-amplitude bedforms created by interaction between eddies and the bed (cf. Allen, 1984), or from the effects of burst-sweep processes on local rates and modes of sediment transport (cf. Cheel and Middleton, 1986). Upflow-inclined, plane-bedded gravel (Fig. 11) is interpreted as a product of deposition in diffuse gravel sheets (cf. Smith, 1990) with well-preserved, longitudinal sediment sorting (cf. Iseya and Ikeda, 1987).

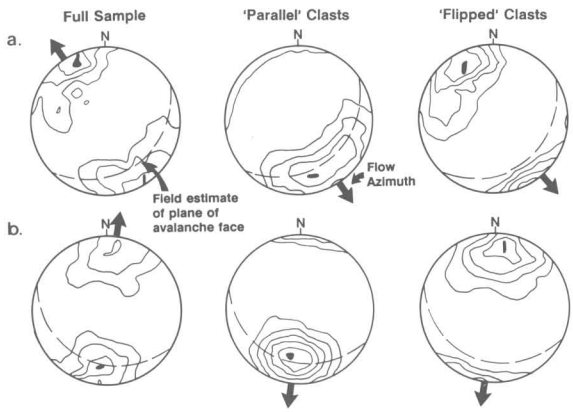

Fig. 12. Examples of gravel fabric plots for southeast-dipping cross-bedded gravel—(a) Q23/1-1—and a large downflow-dipping (south), avalanche-bed of a composite macroform—(b) Q12/1-1aLHS—with "parallel" and "flipped" clasts. All plots are equal-area, lower-hemisphere projections. Statistics in Table 5.

Cross-bedded gravel

Both trough and tabular cross-bedded gravel are observed within the Harricana complex. Tabular cross-beds are generally in single sets, 3–5 m thick, with foreset beds 0.4–1.0 m thick (Figs. 10e, 11). Trough cross-beds may be in single sets, but more commonly form fining-upward cosets.

Boulders and cobbles, or cobbles and pebbles predominate in cross-bedded gravel, and tabular foreset beds usually exhibit rhythmic grading. A typically rhythmically graded bed starts with bimodal boulder or cobble gravel with a small pebble–granule–sand matrix which commonly exhibits convolute laminations (Fig. 10f). This bimodal unit passes up-sequence to cobble–pebble then pebble gravel which may be openwork or include a small amount of fine matrix (Figs. 10e, 11). Occasionally, matrix-rich polymodal beds replace the rhythmically graded triplet. Clast orientation data (unit Q23/1-1, Table 5; Fig. 12a) suggest that "parallel" clasts were emplaced by sliding down the foreset, whereas *a*(t) "flipped" clasts rolled down the foreset and lodged as imbricate clusters, and *a*(p) "flipped" clasts became reoriented by return eddies to the lee of the foreset (Shaw and Gorrell, 1991). Similar rhythmic grading is observed in some trough cross-beds, and in thick (up to 2 m) tabular cross-beds ex-

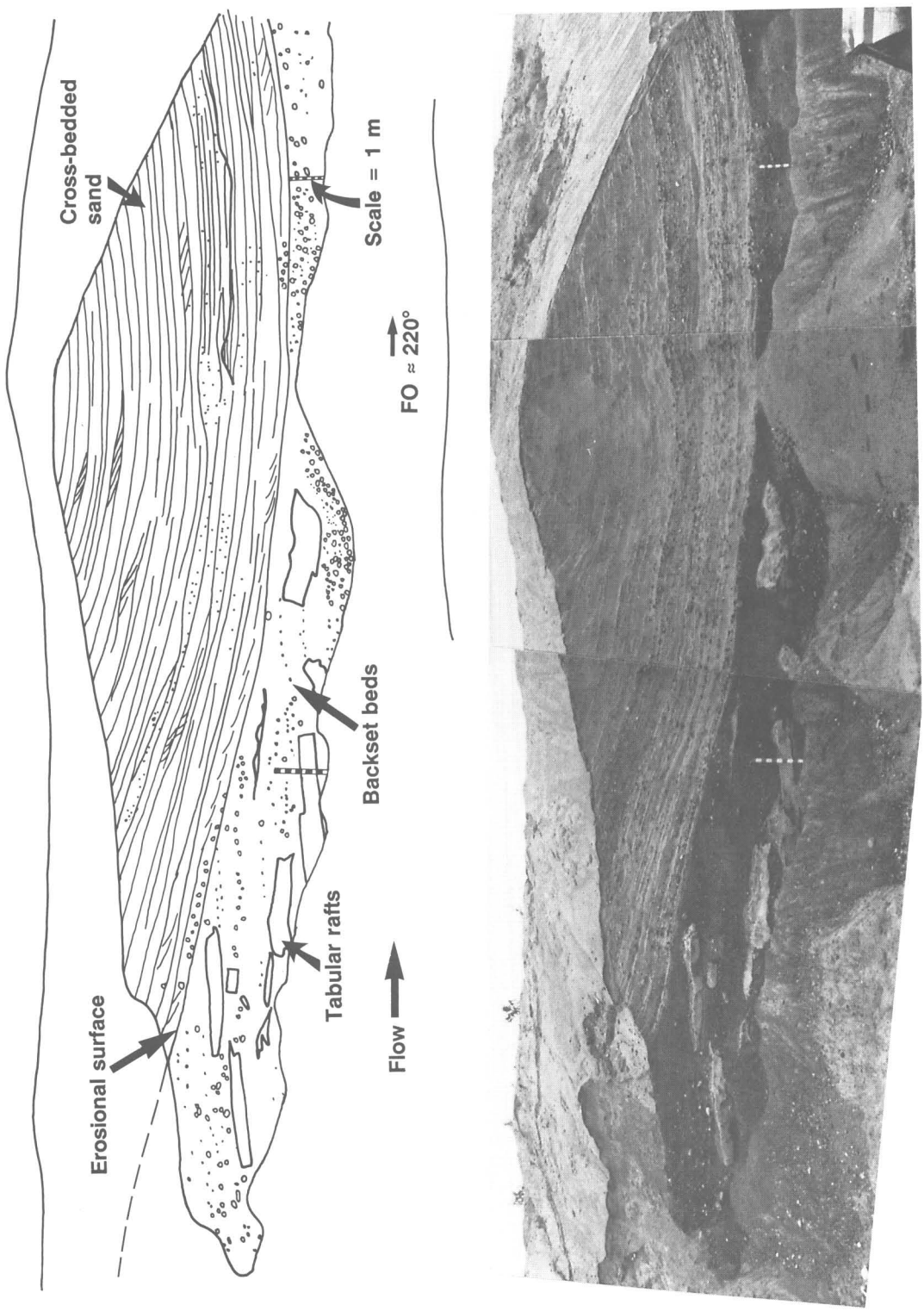

Fig. 13. Large antidune backset beds with tabular rafts of unconsolidated sediment below tabular cross-bedded medium-coarse sand at pit Q20. *FO* is approximate pit face orientation.

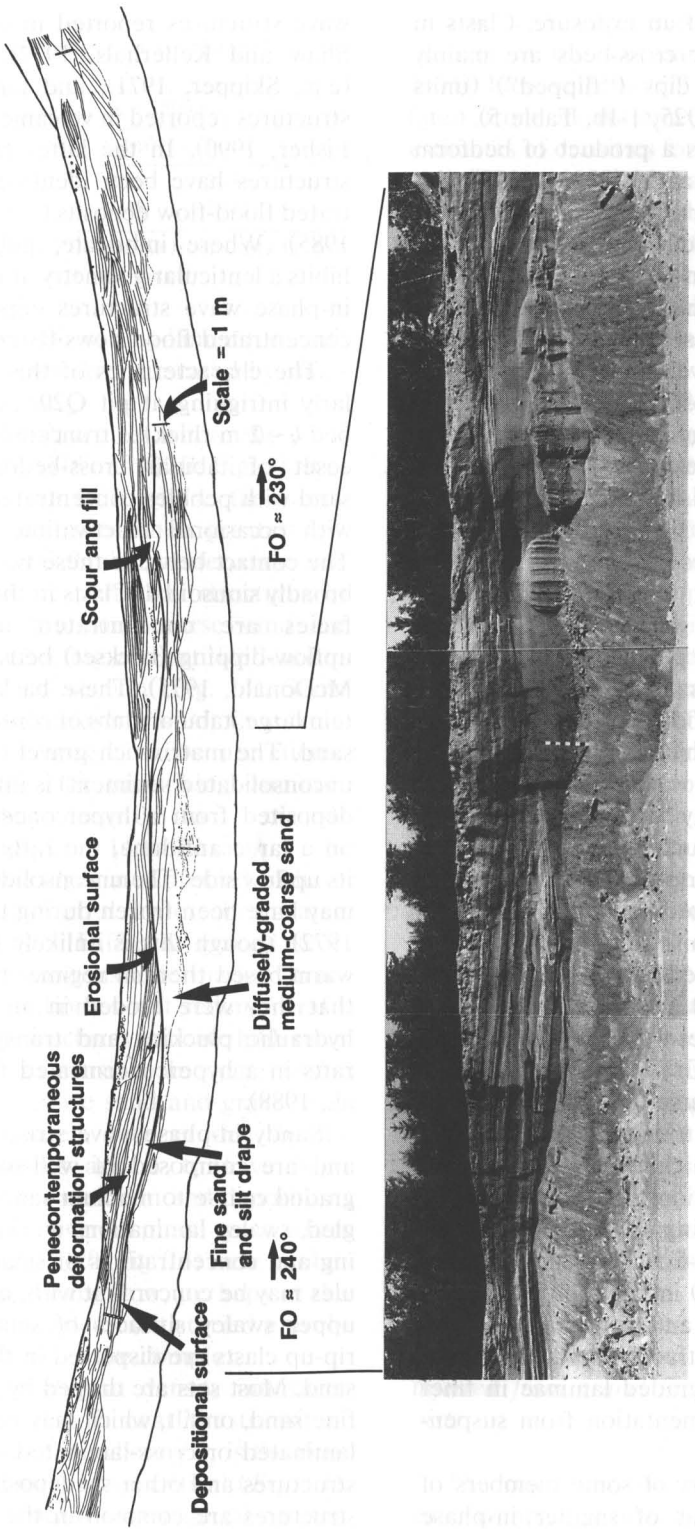

Fig. 14. Sandy in-phase wave structures at pit Q2B. Note: the metre scale is in different locations in the sketch and the photographic panorama, and only a portion of the sketch is shown in the photograph. *FO* is approximate pit face orientation.

tending the full length of an exposure. Clasts in these large-scale tabular cross-beds are mainly *a*(p) with high upflow dips ("flipped") (units Q6/1-2, Q17/1-7RHS, Q25/1-1b, Table 5).

Cross-bedded gravel is a product of bedform migration (cf. McDonald and Vincent, 1972) with mainly traction transport. Longitudinal sorting and lee-side suspension deposition from the return flow of a separation eddy best explain the foreset grading (Shaw and Gorrell, 1991). Such longitudinal sorting is preserved at pit Q23 on the stoss slope of a large gravel dune (Fig. 11). Given the probability of a closed-conduit during the formation of the Harricana complex, flow depths in excess of 10 m are estimated from a dune height of 5 m (McDonald and Vincent, 1972).

Imbricate, polymodal gravel and sandy in-phase wave structures

Imbricate, polymodal gravel is composed of cobbles or boulders with pebbles to coarse sand (Fig. 10c) or of coarse sand and granules with imbricate pebbles (Fig. 10d). Beds are tabular or lenticular and up to 4 m thick. Many finer-grained units exhibit pronounced wavy surfaces, diffusely graded laminae which may be concordant with or truncated by the upper surface, small scour-and-fill structures, and silty rip-up clasts or tabular rafts of unconsolidated sediment (pit Q20, Fig. 13). Clasts in coarser units tend to be concentrated along poorly defined bedding planes (Fig. 10c), forming *a*(t) or *a*(p) imbricate clusters with steeply dipping *ab*-planes (units Q11/1-1 and Q26/1-1LHS, Table 5). Grading in some beds is normal and in others inverse-to-normal.

This facies is inferred to have been deposited from a heterogeneous, highly concentrated dispersion: weak stratification, imbrication, poor sorting, and normal grading are characteristic of hyperconcentrated flood-flow deposits (Smith, 1986). Both *a*(p) and *a*(t) imbrication have been reported in such deposits and attributed to grain-by-grain deposition from traction and suspension (Smith, 1986). Diffusely graded laminae in finer units indicate rapid sedimentation from suspension.

The lenticular geometry of some members of this facies resembles that of smaller in-phase wave structures reported in open-channels (e.g., Shaw and Kellerhals, 1977), turbidity currents (e.g., Skipper, 1971), and larger in-phase wave structures reported in volcaniclastic deposits (e.g., Fisher, 1990). In the latter case, in-phase wave structures have been identified in hyperconcentrated flood-flow deposits (e.g., Pierson and Scott, 1985). Where imbricate, polymodal gravel exhibits a lenticular geometry, it is inferred to record in-phase wave structures deposited from hyperconcentrated flood flows (Brennand, 1994).

The characteristics of this facies are particularly intriguing at pit Q20. A matrix-rich gravel bed ($\sim$ 2 m thick) is truncated by an $\sim$ 8 m thick coset of tabular cross-bedded medium-coarse sand with pebbles concentrated near its base and with occasional reactivation surfaces (Fig. 13). The contact between these two units is sharp and broadly sinusoidal. Clasts in the matrix-rich gravel facies are concentrated along low-angled, upflow-dipping (backset) beds (cf. Banerjee and McDonald, 1975). These backset beds also contain large, tabular slabs of contorted, medium-fine sand. The matrix-rich gravel (with large slabs of unconsolidated sediment) is inferred to have been deposited from a hyperconcentrated flood flow on a large antidune, the rafts coming to rest on its upflow side. The unconsolidated sediment rafts may have been frozen during transport (cf. Shaw, 1972), though this is unlikely given the probable warm-based thermal regime. It is more probable that they were eroded in an unfrozen state by hydraulic plucking and transported as buoyant rafts in a hyperconcentrated flow (cf. Postma et al., 1988).

Sandy in-phase wave structures are lenticular and are composed of well-sorted and diffusely graded coarse to medium sand (Fig. 14). Low-angled, swaley laminations marked by diffuse grading and concentrations of small pebbles or granules may be concordant with, or truncated by, the upper swaley surfaces of sets. Pebbles and silt rip-up clasts are dispersed in the diffusely graded sand. Most sets are draped by medium-fine sand, fine sand, or silt, which may be massive, parallel-laminated or cross-laminated. Microfaults, flame structures and other syndepositional deformation structures are common in the drapes. In places,

Table 6
Estimates of flow depth and velocity for sandy in-phase wave structures

L (m)	$\rho_1 = 1330$ kg m^{-3}		$\rho_1 = 1800$ kg m^{-3}	
	h (m)	U (m s^{-1})	h (m)	U (m s^{-1})
22	2.00	2.21	2.25	3.13
14	1.27	1.76	1.43	2.50

ρ_1, range of hyperconcentrated flood flow from Costa (1988); ρ_2, assumed to be 1000 kg m^{-3} (clear water).

both the drape and the swaley-laminated, diffusely graded sand below are truncated by small scour-and-fill structures.

We noted in-phase structures where the complex widens (pits Q21, Q16 and Q2B, Fig. 3). It is particularly wide at pit Q2B where the sandy in-phase wave structures show their greatest lateral extent in deposits flanking interconnected ridges and beads. These particular structures in diffusely graded medium and coarse sand are stacked and offset, effecting a repetitive lenticular geometry in vertical section (Fig. 14). Some in-phase wave surfaces are erosional; they truncate laminae. Others appear to be accretional and are concordant with underlying laminae. Wave amplitudes range from 0.8 to 1.5 m, and wavelengths (L) range from 14 to 22 m.

In-phase wave structures are inferred to have been deposited by powerful hyperconcentrated flows (cf. Cheel, 1990). Diffusely graded sediments, penecontemporaneous deformation structures, and the preservation of soft-sediment rafts within in-phase wave structures indicate high rates of deposition from suspension. In some cases, diffusely graded or massive sand and gravel may have been first deposited, then eroded, by in-phase waves; conditions appear to have been delicately poised between erosion and deposition. Sand and silt "drapes" over in-phase wave structures (Q2B, Fig. 14 and Q20, Fig. 13) were probably deposited during waning flow, perhaps at the end of events that deposited multistoried gravel–sand couplets elsewhere in the complex.

In-phase waves develop at density interfaces between fluids when flow is near the transition from supercritical ($Fr_d > 1$, where Fr_d is the densimetric Froude number) to subcritical ($Fr_d < 1$). Such conditions may occur in subglacial conduit enlargements (Brennand, 1994), at a grounding line, or at the ice margin (Gorrell and Shaw, 1991). Flow velocity (U) and depth (h) are calculated from measurements of L and plausible estimates of densities for hyperconcentrated flows (ρ_1) (Costa, 1988) and ambient fluid (ρ_2), using equations from Allen (1984, p. 407): $U^2 = gh(\rho_1 - \rho_2)/\rho_1$ and $L = 2\pi h\,(\rho_1 + \rho_2)/\rho_1$), where g is acceleration due to gravity. Paleoflow velocities of 1.7–3.1 m s^{-1} and depths of 1.2–2.3 m are calculated from sandy in-phase waves (Table 6).

Vertically stacked, gravel–sand couplets

Vertically stacked, gravel–sand couplets are common along the length of the Harricana complex (Figs. 13, 15). Sand units are commonly truncated by overlying gravels and appear discontinuous. Generally, pits contain only two to three couplets. However, couplets are more numerous at pits Q16 and Q7 (Fig. 3) where sedimentary assemblages resemble those of subaqueous fans.

Vertically stacked, gravel–sand couplets may result from: (i) temporal or spatial change in sediment supply related to large bedforms and macroforms within a conduit; (ii) spatial change in flow conditions such as the headward growth and capture of conduits and cavities; or (iii) temporal change in flow competence (cf. Brennand, 1994). The latter may result from seasonal melting where supraglacial and subglacial meltwater systems are connected, or to the episodic drainage of supraglacial or subglacial water bodies. At pit Q20 (Figs. 3, 13), 2 m of matrix-rich gravel with backset beds and an in-phase wave surface is overlain by ~ 8 m of cross-bedded medium-coarse sand. This complete sequence was probably deposited during a single meltwater discharge event, possibly a jökulhlaup. Alternatively, Allard (1974) attributed similar gravel–sand couplets in the Harricana complex to annual meltwater discharge cycles.

4.2. Flow dynamics and sediment transport regime inferred from gravel facies and gravel–sand couplets

The coarseness of the deposits in the Harricana complex points to transport and deposition

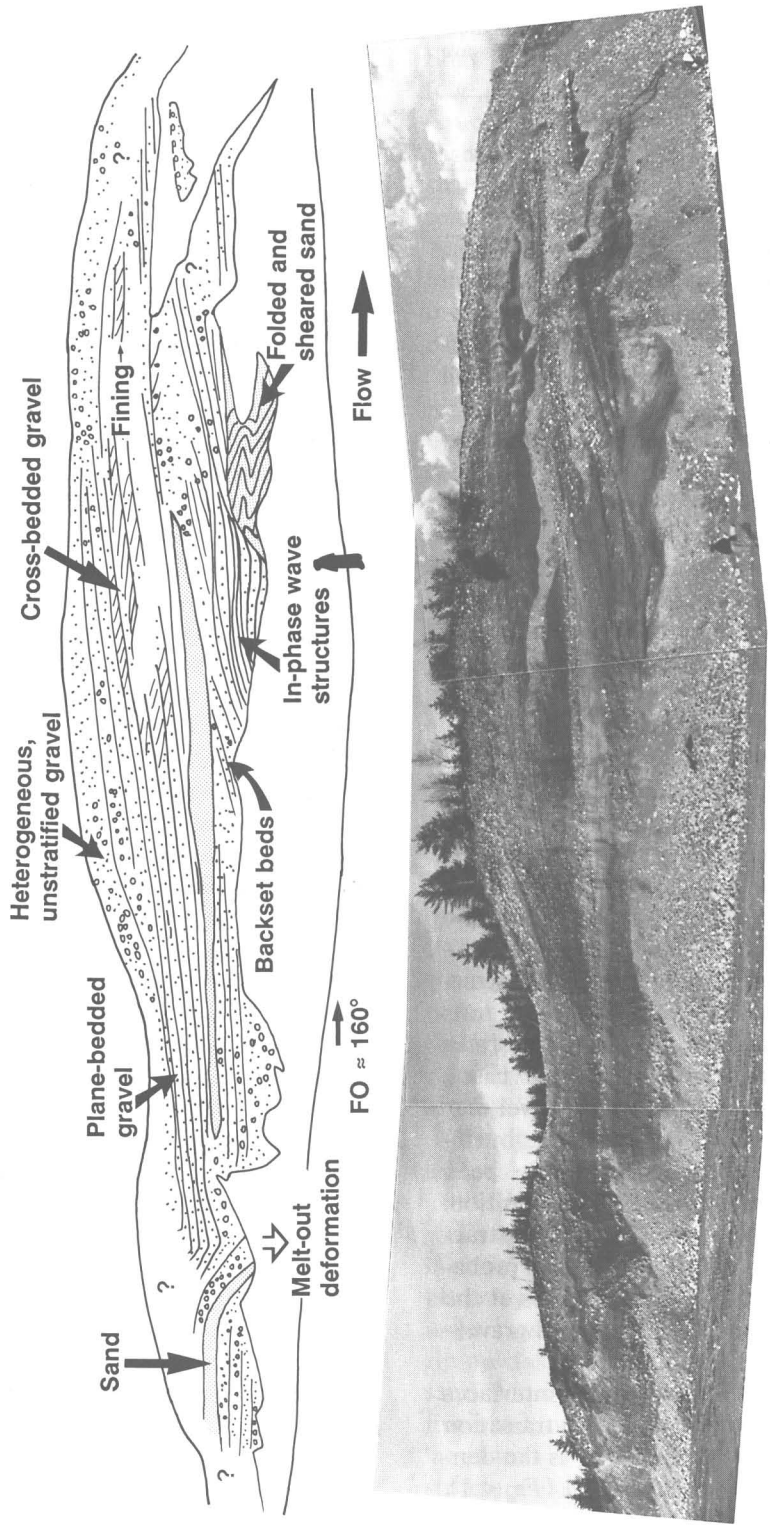

Fig. 15. Composite macroform at pit Q18. Person for scale. *FO* is approximate pit face orientation.

by extremely powerful flows. Rhythmically graded, cross-bedded gravel and longitudinal sorting indicate sediment transport in pulses under shear stresses well above critical (Iseya and Ikeda, 1987). Flipped clasts on avalanche slopes indicate powerful return currents on lee slopes and attest to high primary flow power (Shaw and Gorrell, 1991). High flow power is further indicated by evidence for saltation and even suspension transport of gravel (Johansson, 1976). Gravel–sand couplets also favour extreme magnitude events and unsteady flow.

This inference of high flow power is supported by evidence from finer-grained sediment. Dimensions of in-phase wave structures give estimated flow velocities of about 3 m s^{-1}, and unconsolidated slabs and massive or diffusely graded sand indicate hyperconcentrated flows with extremely high transport and deposition rates. Local conduit enlargement was evidently important in controlling sedimentation, especially in creating internal waves and in-phase bedforms. Besides the evidence for extreme flow, draped beds in silt indicate periods in which flow virtually halted.

4.3. Macroforms

Gravel and sand facies in the Harricana complex are arranged into macroforms, or large-scale bedforms, which scale with conduit width. Three macroforms are identified: composite, oblique-accretion avalanche bed, and pseudoanticlinal.

Composite macroforms

Composite macroforms containing numerous gravel facies were confidently identified only in excellent exposures (pits Q23, Q18, and perhaps Q12, Figs. 11, 15, 16). Their architecture includes distinct stoss and lee sides. Stoss slopes dip at about 5°–10° and foresets lie close to the angle of rest for sand and gravel. They are inferred to have formed incrementally in conduit enlargements (Fig. 17a).

A portion of a composite macroform is exposed in a 100 m long, flow-parallel exposure at Q23. The complex at this site is relatively narrow with a high crest and steep side slopes. Rhythmically graded cross-beds are truncated by an up-

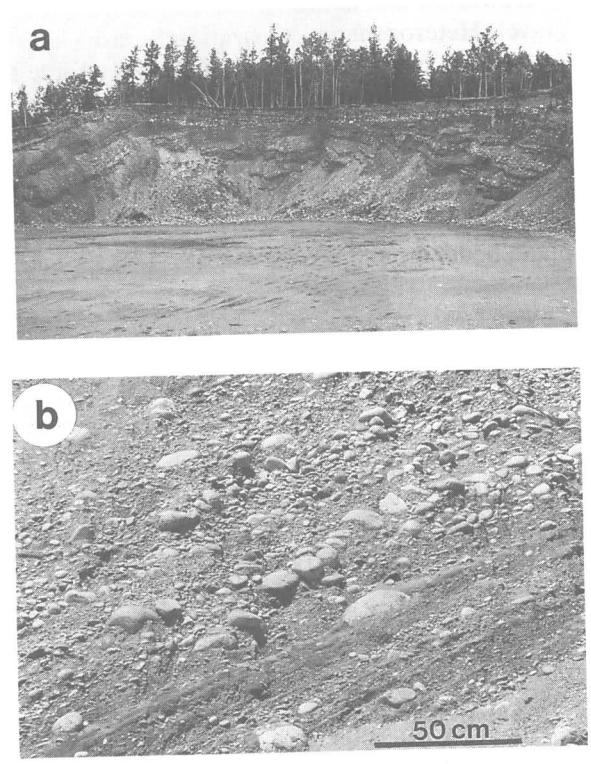

Fig. 16. (a) Downflow-accretion, avalanche-beds of a composite macroform at pit Q12. Section is ~10 m high. Flow out of face. (b) Close-up of avalanche beds at pit Q12 showing "parallel" and "flipped" clasts.

flow-dipping erosional surface, with conformable plane-bedded, stoss-side gravel passing downflow into cross-bedded gravel. The lower cross-bed set is about 5 m thick. Stoss-side beds are inclined at about 5°–10°, show subtle convex-up bedding planes, and are longitudinally sorted (Fig. 11). Small pebbles in these beds were deposited from suspension or saltation, whereas larger pebbles and cobbles were transported as bedload (unit Q23/1-2, Table 5).

The exposed macroform architecture represents two superimposed large dunes. Preserved stoss-side stratification with longitudinal sorting and suspension or saltation deposition of pebbles imply rapid sedimentation. Graded cross-beds indicate pulsating flow with episodes of intense scour upflow of the dune causing longitudinal sorting.

Downflow and laterally, cross-beds are in finer gravel. Heterogeneous, unstratified gravel lateral to the core of the macroform (Q23/2-1, Table 5) was variously deposited from bedload or suspension. A debris-flow deposit with a pronounced flow nose indicates slope instability on the northeast flank of the macroform (Fig. 11). Massive gravel interfingers with massive, cross-bedded and plane-bedded medium to fine sand on this flank. Sandy, matrix-supported diamicton with shear planes and folds is exposed in the lowest and most lateral exposures. The lateral deposits are displaced by numerous normal faults.

Lateral fining and the instability shown by the faulting and debris flows are thought to represent late-stage depositional conditions when conduit widening caused removal of lateral support and flow was much less powerful than when the com-

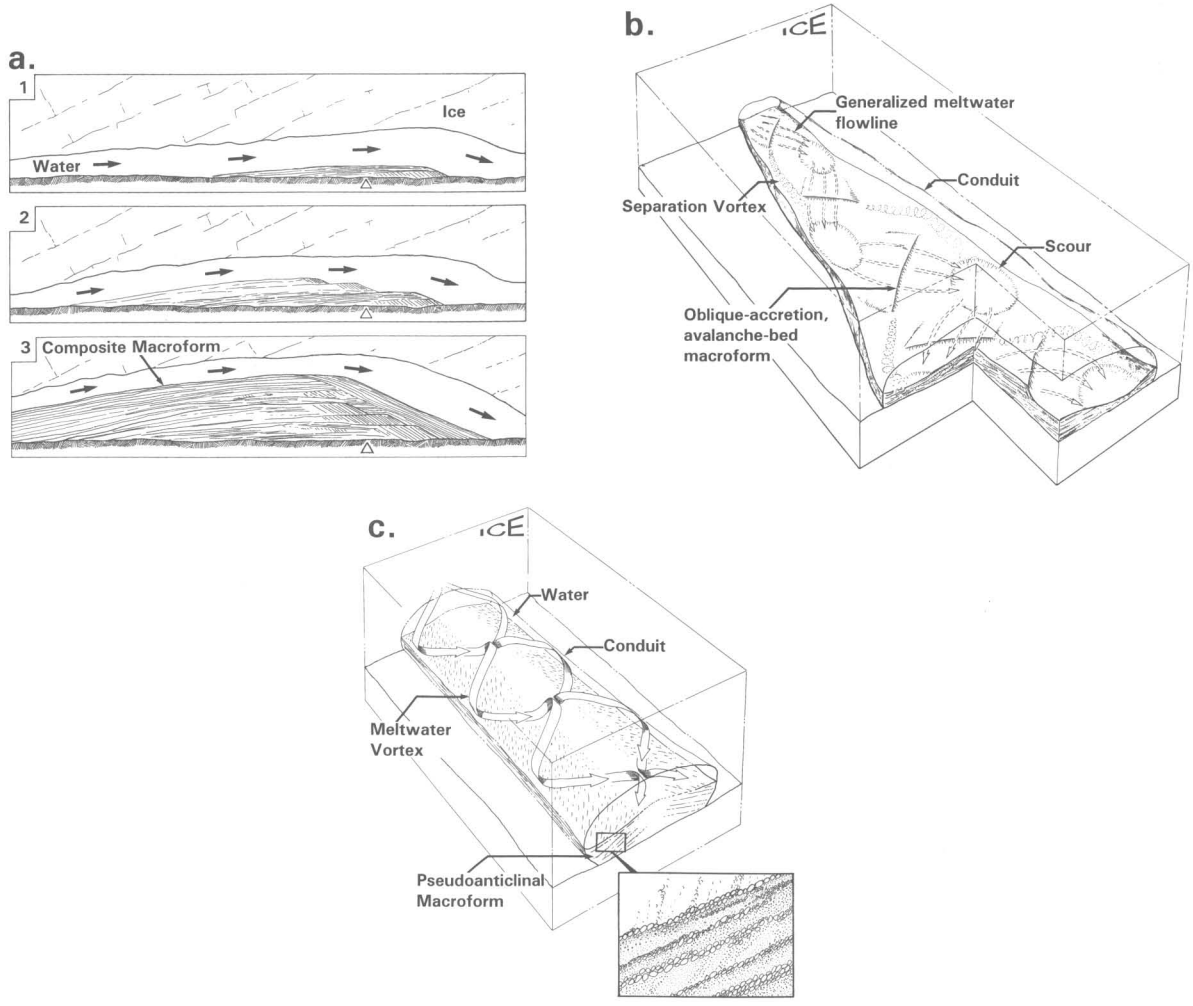

Fig. 17. (a) Incremental formation (stages 1–3) of a composite macroform in a conduit enlargement. Over time and with sedimentation the ice roof melts up and back. (b) Formation of oblique macroforms resulting in oblique-accretion, avalanche beds. These forms are related to the combined effects of separation vortices generated to the lee of the bedform and convergence scours. Alternating, oblique-accretion avalanche beds are expected where oblique macroforms migrate into conduit enlargements. (c) Formation of pseudoanticlinal macroforms related to paired vortices of similar power in conduit segments of uniform width.

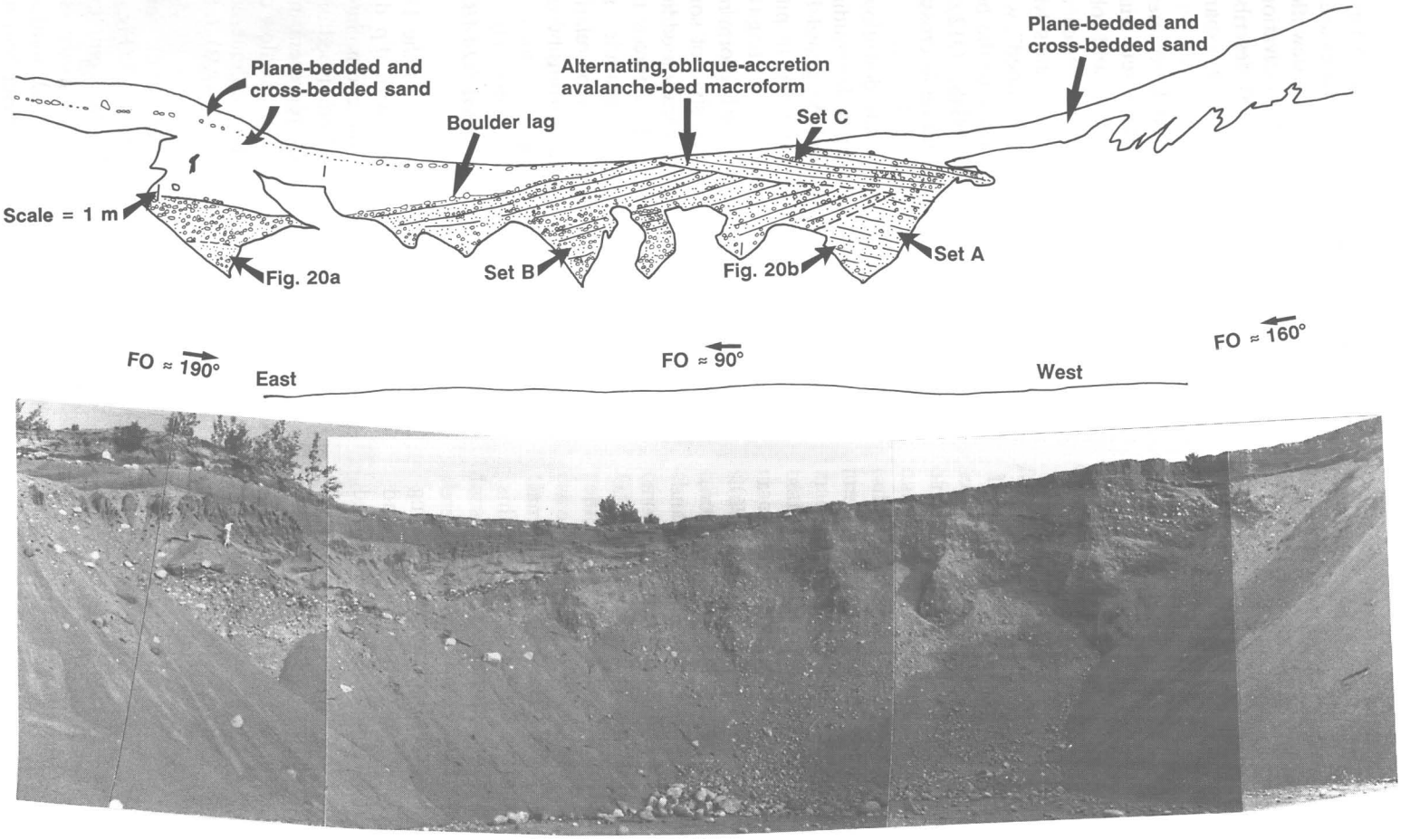

Fig. 18. Alternating, oblique-accretion, avalanche-bed macroform at pit Q3. Flow into face. *FO* is approximate pit face orientation.

posite macroform was active (cf. Shaw, 1972; McDonald and Shilts, 1975). The heterogeneous gravel represents intermediate flow conditions between those for dune formation and those during the waning stages of conduit flow.

A second macroform was exposed in part of segment 4 of the Harricana complex west of Lac Paradis (pit Q18). About 9 m of alternating gravel and sand beds dip upflow (Fig. 15). The gravel is cross-bedded and plane-bedded, the sand cross-bedded and cross-laminated. The upper part of the sequence fines downflow from predominantly gravel to predominantly sand. Folding and shearing of the lowermost sand beds in the direction of meltwater flow suggest high drag forces by the fluid on the bed. These deformed beds are truncated and overlain by in-phase wave structures. Besides the folding and thrust faults, normal faults and subsidence deformation in the proximal part of the section indicate melt-out of buried ice.

The architecture of these deposits indicates backset beds formed at a flow expansion in a subglacial conduit enlargement (Johansson, 1976). Downflow fining also supports this interpretation, as do the in-phase waves. The cross-bedding and cross-lamination can be pictured as resulting from dunes and ripples climbing the stoss slope of a much larger bedform. It may well be that the larger bedform was associated with paragenesis whereby the cavity melted upwards by thermal erosion as sedimentation raised its bed. If this were the case, the extremely high shear stresses necessary to fold and thrust the lower sands were probably related to a period of rapidly increasing discharge during which velocity gradients and shear stresses were high until melting increased the cross-sectional area. Alternating sand and gravel beds also mark highly unsteady flow. Relatively high velocities and attendant low pressure upflow from the expansion would have promoted ice invasion in this part of the conduit. Melting of this ice, following deposition of sand and gravel, accounts for the faulting and subsidence in proximal areas of the macroform.

A third composite macroform, also composed mainly of cross-bed sets, is exposed at the distal end of an apparently streamlined mound in segment 10 (pit Q12; Fig. 16a). The mound is one of two in this segment, each about 5 km long. Sets are 0.5–2.0 m thick. Set boundaries are convex up in transverse section and dip downflow. Truncated set boundaries record reactivation surfaces. Rust (1984) and Baker (1978) described similar macroforms as longitudinal or expansion features.

Cross-beds of polymodal, framework-supported gravel alternate within sets with beds of granules with dispersed pebbles and cobbles (Fig. 16b). Gravel clasts in the cross-beds are either "parallel", with *a*-axes or *ab*-planes lying in the plane of the cross-beds, or "flipped", with *a*-axes and *ab*-planes at a high angle to the beds (units Q12/1-1aLHS, Q12/1-1aRHS, Q12/1-1bLHS, Table 5; Fig. 12). Some granule cross-beds are inversely graded.

The convex-up bedding and downflow dip suggest leeside accretion on a longitudinal ridge composed of smaller, climbing gravel bedforms. The scour and sorting may point to pulsed erosion and longitudinal sediment sorting (Iseya and Ikeda, 1987) or superimposed bedform migration. High shear stresses for this style of sorting and powerful return flows in separation eddies, which flipped gravel clasts, point to vigorous transport. The inverse grading of the granules may also indicate high rates of delivery of relatively fine sediment to slip faces and sorting by dispersive stresses during avalanching.

Oblique-accretion, avalanche-bed (OAAB) macroforms

Some large-scale cross-beds in the Harricana complex form in single sets with dip directions oblique to general flow directions interpreted from the landform axes and other bedforms. It is clear that these cross-beds represent migrating bedforms with crests oblique to the flow direction (Fig. 17b). Hence, we call them oblique-accretion, avalanche-bed macroforms (OAAB) (cf. Brennand, 1994).

Three superimposed sets with erosional boundaries extend through pits Q3 (Fig. 18) and Q2A. The axis of the Harricana complex in the vicinity lies north to south and, in succession, the cross-beds dip: southwest (set A), southeast (set B), then southwest (set C). Foreset beds are from

0.5 to 1.0 m thick. Some foresets contain polymodal gravel with clusters of flipped clasts at high angles to the bedding planes. Others are rhythmically graded from relatively matrix-rich and bimodal clast-supported gravel with a cobble and pebble framework and coarse sand matrix, to openwork pebbles, to openwork granules. The large-scale cross-bed sets are overlain by about 6 m of plane-bedded and cross-bedded granules and coarse sand with dispersed pebbles.

Similar macroforms are observed at pits Q4 and Q21. In both cases, only a single OAAB set was observed and paleoflow direction estimates from gravel fabrics were away from the crest of the Harricana complex (down the avalanche face) and obliquely downflow (units Q4/3-3 and Q21/5-1, Table 5). Clasts were either "flipped" or "parallel" to the plane of the avalanche face.

Oblique macroforms must have resembled alternating bars, similar to those which form as braided channels evolve from straight channels (cf. Ashmore, 1991, fig. 3a). Such bars or gravel sheets are located downstream from flow convergence scours (Fig. 17b). A steep avalanche face at the forward margin of the subglacial oblique bars distinguishes them from braided stream forms. Generation of a vortex at the slip face may have contributed to the scour upstream from the next-but-one oblique bar (Fig. 17b). Jaeggi (1984) showed that alternating bars in rivers develop in poorly sorted bed material when the shear stresses are well above critical for all sizes. The large-scale bedforms, flipped clasts and bimodal and graded gravels also speak for powerful flow conditions in the conduit.

Migrating alternating bars climbed over preceding bars to produce net accretion. This most likely happened at a flow expansion in a conduit enlargement, where the rate of scour decreased and the forward migration of the bedforms slowed (Fig. 17b). In the final stage of deposition, lower flow power resulted in finer-grained sediment deposited on horizontal beds and in dunes which climbed over the macroform.

Pseudoanticlinal macroforms

Pseudoanticlinal macroforms are broad, low-angled, arched structures scaling with the width of the complex (Fig. 19; Brennand, 1994). Only one of these macroforms was identified with certainty (pit Q8, Fig. 19), though beds at pit Q19 may also form one limb of a pseudoanticlinal macroform. The complex is relatively narrow at both of these locations (Fig. 3). At pit Q8, the macroform is composed of heterogeneous, unstratified cobble and pebble gravel (Fig. 19). Paleoflow direction estimated from imbricated clast clusters is downflow and convergent on the crest of the macroform or Harricana complex (unit Q8/1-1LHS, Table 5). Deposition from tractional rolling, suspension and saltation are inferred from clast orientation relative to the paleoflow direction (unit Q8/1-1LHS, Table 5).

The formation of a pseudoanticlinal macroform with crest-convergent fabric is inferred to be the product of secondary currents or vortices in a

Fig. 19. Low-angled, pseudoanticlinal macroform at pit Q8. Arrow is location of fabric from unit Q8/1-1LHS (Table 5). Flow into face. Section is 5.5 m high.

narrow, geometrically uniform conduit (Fig. 17c) (cf. Rouse, 1961; Brennand, 1994).

4.4. Macroforms and sedimentary environments: discussion

The macroforms in the Harricana complex give hints on the details of sedimentary processes in large conduits. They are, in part, a product of flow characteristics imposed by the conduit shape (Brennand, 1994). Pseudoanticlinal macroforms result from powerful flows in uniform conduits, whereas composite and oblique accretional macroforms result from reduced flow competence in areas of flow expansion (Fig. 17). Exactly what caused conduit enlargement is not clear, though we may speculate that they were related to prior cavities (Walder and Hallet, 1979; Iken and Bindshadler, 1986; Hooke, 1989, fig. 4) or to increased pressure with increasing discharge and localized flotation of the ice sheet (Gorrell and Shaw, 1991).

Once formed, macroforms influenced large-scale flow structures, creating an interaction between the flow and the bed. They must also have controlled sedimentary characteristics by acting as sediment traps for large clasts. Consequently, with transport distances constrained by the distance between macroforms, clast characteristics are most likely to have been controlled by local flow dynamics and transport regime, supporting earlier conclusions. As well, there must have been a constant supply of sediment to the complex from lateral sources.

4.5. Subaqueous fan and grounding-line assemblages

Plane-bedded and cross-bedded coarse sand and granules lie to the side of esker deposits at pits Q2A and Q3. Inclined beds in fine sediment at pit Q4 include scours filled with diffusely graded or massive medium sand with dispersed pebbles, plane-bedded and cross-bedded sand, and diffusely graded sand with some in-phase wave structures and silt drapes. Glaciolacustrine, parallel-laminated, cross-laminated and massive fine sand with silt and clay overlie these deposits.

Fining-upwards gravel to coarse sand beds (0.1–1.0 m thick) and gravel to medium sand couplets at pit Q7 dip gently downflow. These sediments are exposed within a lobe superimposed on the Harricana complex. The gravel units are plane-bedded, cross-bedded or massive. The coarse sand is mainly massive, with dispersed pebbles, or plane-bedded. Distally in the lobe (pit QC) the sediment fines and is mainly plane-bedded and cross-bedded medium to coarse sand.

Flanking deposits at pit Q16 contain six couplets of gravel and sand that pass distally into plane-bedded and diffusely graded medium to coarse sand. The gravel in the couplets is polymodal and clast-supported and the sand is plane-bedded, cross-bedded and diffusely graded. Paleoflow directions were oblique to the axis of the complex (Figs. 8, 9).

Each of the sites under discussion contains sedimentary sequences typical of subaqueous fans (Gorrell and Shaw, 1991). The lateral position of the sediment, its superimposition on the core deposits of the complex, inclined strata, and oblique paleoflow directions are also as expected for fans. Distal fining and lateral position suggest that meltwater spilled out from the main conduit either at a grounding line or into a lateral cavity (Gorrell and Shaw, 1991). Outpouring of sediment-rich submerged jets into less dense standing water accounts for the high sedimentation rates. Scours, massive and diffusely graded sand, and in-phase waves may all have resulted from submerged hydraulic jumps formed where supercritical jets became subcritical (Gorrell and Shaw, 1991).

The fining-upwards sequences, gravel–sand couplets and scoured surfaces indicate unsteady flow. Extreme low flow is indicated by silt drapes. Given that massive and diffusely graded sands were probably deposited quickly (in a matter of minutes or, at most, hours) from suspension, individual couplets or graded units represent single flow events of short duration. The outbursts imply that water was forced outwards when water pressures in the conduit were high. Such high water pressures imply sudden increases in discharge—either by release of stored water in cavities or lakes, or by increased melting at the ice

Table 7
Stratigraphic correlation for Abitibi–Timiskaming and surrounding areas as proposed in the literature

MOOSE RIVER BASIN[1,2] Skinner (1973) Shilts & Wyatt (1988)	TIMMINS TO MOOSE RIVER, NORTHERN ONTARIO S. L. Smith (1992)	MATHESON AREA[1] McClenaghan et al. (1988, 1992) McClenaghan (1989) Steele et al. (1989)	ABITIBI-TIMISKAMING WEST OF HARRICANA COMPLEX[1] Veillette (1986, 1989)	EASTERN JAMES BAY LOWLANDS WEST OF HARRICANA COMPLEX[1,3] Hardy (1976, 1977, 1982)	TIMISKAMING TO JAMES BAY LOWLAND EAST OF HARRICANA COMPLEX[1,3] Veillette (1986, 1989) & Hardy (1976, 1977, 1982)
TERRESTRIAL	TERRESTRIAL	TERRESTRIAL South of Tyrrell Sea limit	TERRESTRIAL South of Tyrrell Sea limit	TERRESTRIAL	TERRESTRIAL
TYRRELL SEA	TYRRELL SEA			TYRRELL SEA	TYRRELL SEA
GLACIAL LAKE BARLOW-OJIBWAY	GLACIAL LAKE BARLOW-OJIBWAY	GLACIAL LAKE BARLOW-OJIBWAY South of Cochrane limit	GLACIAL LAKE BARLOW-OJIBWAY	GLACIAL LAKE BARLOW-OJIBWAY	GLACIAL LAKE BARLOW-OJIBWAY
	SURGING LOBE or ICE STREAM? **130° ? (SE)** *Striae, no till*				
KIPLING TILL **SW, S, W** *Till fabrics; flute orientations; striae on boulders in and below till; composition*	COCHRANE TILL **175° -150° (SE)** *Geochemistry; pebble lithology; limited striae; 1 till fabric*		COCHRANE TILL **SW, S, SE** *Abundant Paleozoic carbonate; landform distribution: flutes*	COCHRANE TILLS **S-ENE** *Bedrock erosion marks; drumlinoids; flutings; abundance of Paleozoic carbonate*	COCHRANE TILLS **S-ENE** *Bedrock erosion marks; drumlinoids; flutings; abundance of Paleozoic carbonate*
FRIDAY CREEK SEDIMENTS **Southward** *Paleocurrents from laminated sand*	BARLOW-OJIBWAY FORMATION		GLACIAL LAKE BARLOW-OJIBWAY	GLACIAL LAKE BARLOW-OJIBWAY	GLACIAL LAKE BARLOW-OJIBWAY
ADAM TILL **SW-SSW** (? early phase) *Striae on boulders in and below till; till fabrics*	MATHESON/ADAM TILL (TILL I) **Upper: 190° -165° (S)** **Lower: ~210° (SW)** *Geochemistry; pebble lithology; limited striae; 1 till fabric*	MATHESON TILL **Upper felsic till: 154° -170° (SE)** **Lower mafic till: ~240° (SW)** *Striae; streamlined bedforms; till fabric; geochemistry; heavy mineral composition; pebble lithology*	MATHESON TILL **Upper: 130° -170° (SSE)** *Striae; landform distribution: eskers, moraines; rare Paleozoic carbonate* **Lower: 180° -220° (SSW)** *Striae; landform distribution: drumlins, crag & tail features; till distribution relative to topography; rare Paleozoic carbonate* *Note: lack of differential weathering of surfaces; some intermediate striae*	SANDY TILL **SSE** *Bedrock erosion marks; esker distributions*	NEW QUEBEC TILL **SW-S** *Streamlined landforms; striae; no carbonate in matrix*

CAPITALS: DEPOSIT. **Bold: inferred ice-flow direction.** *Italics: evidence used to infer ice-flow direction.* Vertical double line within table: divides proposed stratigraphies west and east of the Harricana complex. Vertical thick line within table: proposed timing of deposition of the Harricana complex, and split of Labradorean sector of the Laurentide Ice Sheet into Hudson and New Quebec ice masses (Hardy, 1976); associated with upper part of Matheson till only (Veillette 1986, 1989). Vertical dashed line within table: some authors propose that Kipling and Cochrane tills are correlated based on core stratigraphy, till composition and ice-flow indicators (cf. Skinner, 1973; Veillette, 1989, 1990; Smith, 1992); others suggest that Kipling till is correlated to regionally extensive Severn and Sky Pilot tills of Ontario and Manitoba and therefore not equivalent to the Cochrane till (cf. Thorleifson et al., 1993).

[1] In all cases where streamlined landforms have been used as evidence of ice-flow direction, the implicit assumption is that they were a product of direct glacial action, and therefore represent sustained ice-flow directions. This assumption is currently under debate (cf. Shaw, 1994).

[2] Till units defined on the basis of stratigraphic position, composition and relative amino-acid chronology (Alle/Ile ratios). Approximate orientation of striae and till fabric plotted and tentatively correlated. Often similar orientations were presented as an amalgamated single orientation; full statistical rigour was not applied. Paleocurrent directions stated; data not displayed.

[3] Bedrock erosion marks implicitly assumed to be formed by direct glacial erosion, although some appear to be morphologically similar to meltwater erosion marks, or s-forms, reported by Kor et al. (1991).

surface. Clay in the associated glaciolacustrine sediment and silt drapes in fan sediment suggest periods with minimum discharge. It is probable that the periodic discharge relates at least in part to seasonal or weather conditions. Thus, supraglacial sources for meltwater most likely provided a large proportion of the total conduit discharge. This conclusion on meltwater source is of fundamental importance to later discussion.

5. Discussion: stratigraphic context, landform associations and implications for ice-sheet hydrology and dynamics

Geomorphology, clast characteristics, paleoflow direction estimates, and sedimentology of the Harricana complex, between latitudes 48°N and 50°N, favour an origin by synchronous deposition of a subglacial esker in a continuous, closed conduit (Table 1). Some subaqueous fans rest on, or lie lateral to, these primary deposits. Such fans may have been deposited in subglacial cavities during esker formation, or were superimposed over esker deposits (cf. Wilson, 1938) at a grounding-line or in an ice-marginal position during ice retreat or downwasting. Our view, that most of the sediments of the Harricana complex are eskerine and approximately synchronous, must be rationalized with event-sequences determined from adjacent stratigraphy and landforms; it is important that local and regional interpretations are consistent.

5.1. Stratigraphic context

Regional correlations from the literature, together with reported ice-flow directions and evidence used to infer those directions, are presented in Table 7. The Adam, lower Matheson and New Quebec tills have been attributed, on the basis of till composition, fabric and striae, to southwest flow of Labrador sector ice, related to a northern Quebec ice centre (Thorleifson et al., 1992, 1993). This ice would have flowed across the area now occupied by the Harricana complex (Veillette, 1986). The southwest flow shifted to the south-southeast around the time of deposition of the upper parts of the Matheson and Sandy tills (cf. Veillette et al., 1989; McClenaghan et al., 1992). Although some intermediate striae between southwest and south-southeast are reported, cross-cutting southwest and south-southeast striae are more common, and no differential weathering of these striae is apparent (cf. Veillette, 1986). Veillette (1986) concluded that the area was not deglaciated between the two erosional events. This reasonable conclusion raises the equally reasonable question: Why are striae indicating intermediate flow directions between the principal directions not common? An ice sheet cannot be expected to switch flow direction abruptly; intermediate striae are to be expected. We return later to this fundamental question.

The change in flow direction may represent the break-up of the Labrador sector of the Laurentide Ice Sheet into the smaller New Quebec and Hudson ice masses, with time-transgressive deposition of an interlobate Harricana moraine between them (cf. Hardy, 1976; Veillette, 1986, 1989). Veillette (1990) favoured this break-up and attributed it to drawdown of ice resulting from rapid flow over a deforming substrate in the Great Lakes region. He argued that thinner ice, caused by drawdown, and calving into an ice-dammed lake produced a reentrant in the ice margin which became a focus for sedimentation. The Harricana complex was said to have been deposited along the path of the reentrant as it moved northwards with the retreating ice front.

This time-transgressive model for the Harricana complex fits many observations well: it explains a linear glaciofluvial complex on the scale of the Harricana deposits, and convergent striae and eskers are to be expected given an embayment cutting deeply into the ice margin. It is also in agreement with explanations for interlobate moraines elsewhere (cf. Punkari, 1980), and it anticipated some modern views on subglacial deformation and ice-sheet behaviour in the Great Lakes region (Hicock and Dreimanis, 1992).

Yet the time-transgressive model does not stand up as well when more detailed evidence is introduced. As noted, ice flow veering between the two principal directions recorded in the area

should have produced intermediate striae at all sites where cross-cutting striae are observed. Progressively younger striae should show anticlockwise rotation. We may argue that the grounded ice sheet did not erode as it changed flow direction, or that it deposited sediment at this time. If either of these processes ensued as the flow direction shifted, there would be no intermediate striae. But, this is a weak argument, dependent on unexplained coincidence. We are encouraged to look for stronger explanations for the rarity of intermediate striae.

The evidence presented here for synchronous deposition of the Harricana complex over its whole length is also at odds with a model which holds that the bulk of the complex was deposited in a migrating embayment. Once again, we are encouraged to seek an alternative explanation for the Harricana complex and to reevaluate the concept of interlobate moraines in general.

5.2. *Landform associations*

Landforms associated with the Harricana complex include the Abitibi Uplands, eskers, moraines, streamlined landforms, and bedrock erosional forms, some of which are shown on Figs. 1 and 2. Much of the Harricana complex is located in a dissected portion of the Abitibi Uplands. Its path is diverted at the margin of the dissected zone south of Val d'Or (Figs. 1, 2). Veillette (1986) attributed this change in orientation of the complex, from south-southeast to southwest, to changing ice flow directions as the ice sheet retreated. He implied time-transgressive formation of the Harricana–Lake McConnell complex. However, the bend may also have resulted from topographic control on hydraulic gradients in the ice sheet (Shreve, 1972).

Fields of streamlined forms adjacent to the Harricana complex (cf. Prest et al., 1968) were interpreted by Hardy (1976) to have formed time-transgressively within 100 km of the retreating ice margin. Excluding the enigmatic Cochrane landforms, streamlined landforms are said to have formed before the Harricana complex (Veillette, 1990). Punkari (1980) drew a similar conclusion for drumlins and interlobate moraines in Finland and others have argued that drumlins preceded eskers (cf. Wright, 1973; Shaw et al., 1989). Brennand and Sharpe (1993) and Brennand and Shaw (1994) infer that eskers relate to ice-sheet dynamics and hydrology inherited from the effects of meltwater outburst events that formed associated streamlined features. This sequence might be important to our discussion given the similarity between the Harricana complex and large eskers. Short eskers to the east of the Harricana complex converge on the complex to the north and diverge from it to the south (Figs. 1, 3). Eskers in a complex, integrated network to the west of the complex converge on the portion of the Abitibi Uplands dissected by anabranching through valleys (Fig. 1). Both sets of eskers were likely formed at the same time as the complex.

These temporal relationships between streamlined forms, eskers and the Harricana complex constrain models of deglaciation. In both the time-transgressive and synchronous models for the Harricana complex, streamlined landforms precede glaciofluvial deposition of the complex and eskers. If the Harricana complex was formed synchronously, then the streamlined forms could not have formed incrementally. Since we favour synchronous formation of the complex, we are obliged to provide a plausible mechanism for formation of streamlined forms when the ice margin lay beyond the southern limit of Harricana deposits. We do this later by way of a regional reconstruction of events that began with the formation of streamlined landforms and culminated in the formation of the Harricana complex and associated eskers.

Compelling evidence that streamlined forms relate directly to ice-marginal landforms adjacent to the Harricana complex would contradict our temporal conclusions and would pose major difficulties for our reconstruction. As it is, there are only a few ice-marginal landforms or deposits in the Abitibi–Timiskaming region or to the north in the James Bay Lowlands (Thorleifson et al., 1993). Most moraines are composed of glaciofluvial sediments (cf. Boissonneau, 1968; Vincent, 1989; Veillette, 1990) and, disregarding the enigmatic Cochrane flutings, they formed later than streamlined forms in the region.

If active Hudson and New Quebec ice masses retreated across subglacial landforms, ice-marginal landforms should be systematically superimposed on subglacial features. This is clearly not the case. As well, the streamlined forms should be clearly related to contemporaneous ice-frontal positions marked by moraines. In reality, there is no obvious correlation between streamlined forms and marginal moraines. Once more, the time-transgressive model does not fit observation.

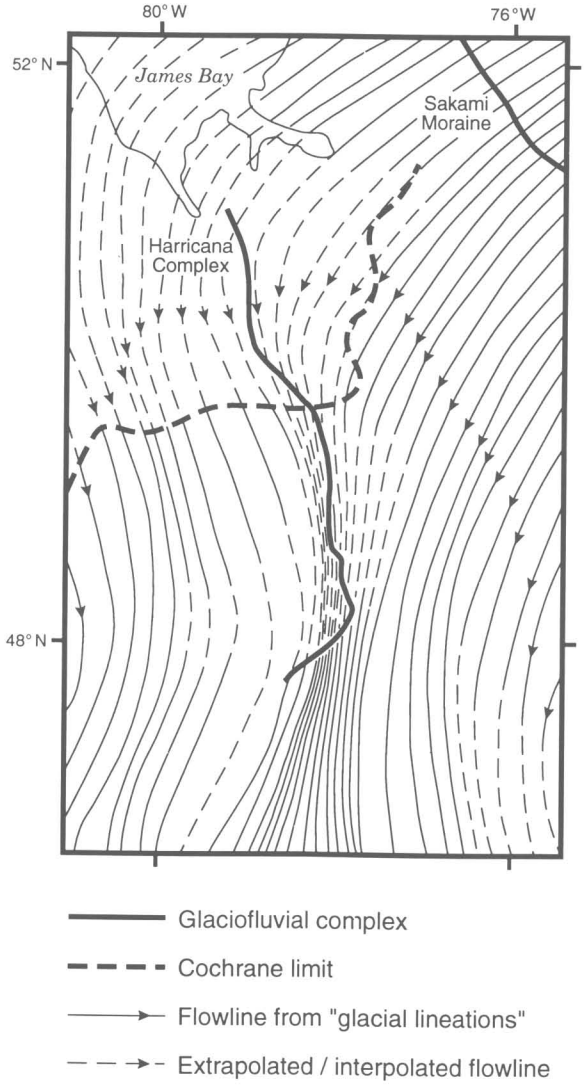

Fig. 20. The position of the Harricana complex with respect to regional flowlines reconstructed from "glacial lineations" (Prest et al., 1968).

The latest striae appear to converge on the Harricana complex at both regional (as far west as Timmins, Ontario; Smith, 1992) and local scales (Veillette, 1986). Some striae are parallel to the Harricana complex (Vincent, 1989) and converge on other large eskers such as the Roulier and Moffett eskers (Veillette, 1986). Local convergence of striae on eskers may be explained by indraw of ice caused by melting at conduit walls (cf. Shreve, 1985; Shilts et al., 1987). This process need not accompany flow in the ice sheet as a whole. Indraw of ice also explains lateral transport of sediment to the Harricana complex. In addition, thermal and fluvial erosion in marginal areas of thinner ice would have eventually resulted in the development of a reentrant at the downflow end of a large conduit.

Regional convergence of striae on the Harricana complex is perhaps more interesting. Whereas Veillette (1986, 1989, 1990) argues that these striae were formed perpendicular to the retreating Hudson ice margin, we find little reported evidence to corroborate active ice-marginal retreat in this region. Southeast of Val d'Or, striae appear to diverge at the margin of the breach in the Abitibi Uplands (Fig. 2), a similar divergence to that shown by the eskers (Fig. 1). This divergence may be attributed to topographic funnelling and reorientation of equipotential contours in the ice sheet where it flowed over the Abitibi Uplands. Bedrock erosion marks, or s-forms (Kor et al., 1991), and rat-tails have been reported to parallel striae and flutings in the region (e.g., Veillette, 1986, 1990).

5.3. An alternative model for the Harricana complex

In view of the accumulated evidence, it is timely to reconsider the Harricana complex in a regional context. Striae on either side of the complex converge on it. Veillette (1986) noted that older striae show a northeast to southwest orientation, and cross-cutting by northwest to southeast striae is only observed to the west of the complex. Clearly, southeast flow was confined to the west of the complex and, since it was supported by ice on both sides, ice flow to the

east must have been from the northeast. This change in flow may have been a response to migrating ice divides or to more local effects such as calving bays. Either change must have been abrupt or, alternatively, striae were not formed during the transition. Since ice divides are expected to shift much more slowly than the few weeks it takes to form centimetre-scale striations, abrupt change rules out shifting ice divides as an explanation for the shift in flow direction. Moreover, simultaneous deposition of the Harricana complex in a continuous conduit contradicts deposition in migrating embayments in the ice margin as an explanation for the bulk of the Harricana complex.

A satisfactory alternative explanation is available if we relate the Harricana complex and associated striae and eskers to the formation of streamlined landforms which preceded them. Punkari (1985, fig. 28) plotted flowlines for several "ice-lobes" in Soviet Karelia. The flowlines for adjacent lobes do not cross, but converge on interlobate zones. Heikkinen and Tikkanen (1989) also showed that flowlines constructed from drumlins and flutes for adjacent lobes do not cross, and drumlins are absent in interlobate zones. Since flowlines were not cross-cutting and drumlins do not occur in interlobate zones, drumlin-forming flows of adjacent lobes were active at the same time.

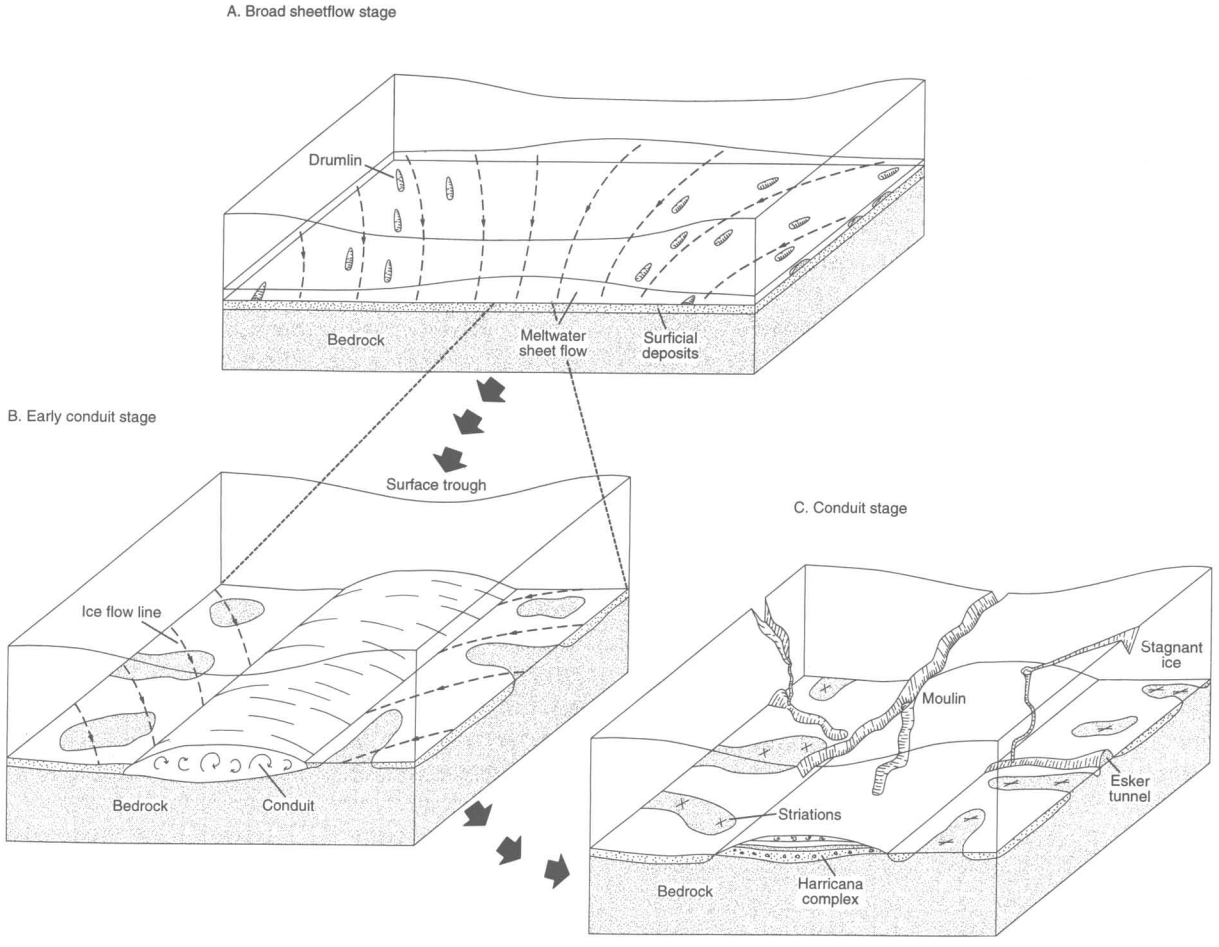

Fig. 21. Proposed sequence of events leading to the formation of the Harricana complex. See text for explanation.

We may construct a similar flowline diagram from streamlined forms (excluding the Cochrane flutings) in the vicinity of the Harricana complex using Prest et al. (1968) (Fig. 20). The flowlines are drawn assuming equal discharge per unit width in the northern part of the map. Although a variety of plausible flow fields could be drawn in the immediate vicinity of James Bay where there is little data, the flow pattern is well constrained elsewhere. The most striking feature of the flowline map is the flow convergence south of James Bay in the vicinity of the Harricana complex. This convergence may well be the key to the origin of the complex. The flowlines on either side of the convergence are confluent rather than cross-cutting and, as is the case for areas of flow convergence in Finland, streamlined forms are not mapped where the flowlines are most crowded in the throat of the convergence.

Streamlined landforms and bedrock erosional features, which provide the data for the flowline map, may be products of meltwater sheet floods (cf. Shaw et al., 1989; Kor et al., 1991). We use this interpretation as the basis for an explanation of the Harricana complex. Those interested in a justification of this assumption are referred to the papers cited above.

If it can be assumed that the flowlines of Fig. 20 are for subglacial meltwater flow beneath the Laurentide Ice Sheet, the convergence would have been a zone of extremely high discharge, with discharges per unit width about twice the average if flow depths had been uniform. But, depths are unlikely to have been uniform because enhanced meltwater erosion of the ice in the convergence zone would have increased the gap width between the ice and the bed. Discharges in this zone would have been relatively high. In the meltwater hypothesis, drumlins, flutings and bedrock erosional marks formed during this sheetflow stage. Ice would have flowed with a lateral component towards the meltwater convergence, replacing ice that had melted. The surface of the ice sheet above the convergence zone would have been drawn down, creating an extensive trough there. In time, as the glacier reattached to its bed, the sheet flow phase would have drawn to a close. At this stage, surface meltwater would have continued to flow into the trough and would have eventually made its way through moulins to the ice bed (Shoemaker, 1992). At the bed, it would have flowed towards the ice margin along the zone of low pressure beneath thinner ice. Consequently, a major conduit is expected to have been maintained beneath the surface trough in order to evacuate meltwater from supraglacial and subglacial sources.

How do our observations fit this reconstruction of events? In other words: How well does our hypothesis explain the facts? In the reconstruction (Fig. 21), the oldest striations, indicating flow from the northeast, formed prior to the sheet flood. They correspond to a widely reported southwestwards flow of Labradorian ice from an ice centre in northern Quebec (Veillette, 1986; Thorleifson et al., 1992). In our model, streamlined forms and bedrock erosional marks were created by the sheet flood itself (Fig. 21A). Thinner ice and a surface trough resulted where meltwater flowlines converged. This caused ice flow to converge beneath the trough when the ice sheet reattached to its bed. Since the ice was separated from its bed when flow direction shifted, striations on lower ground are expected to cut across older ones without any striae of intermediate trend. Intermediate striae may have formed at higher elevations if the ice remained grounded there. Debris was transported towards, and meltwater flowed towards this trough, necessitating an early conduit (Fig. 21B). Thus, convergent flow accounts for both the cross-cutting striae and the lateral transport of debris deduced from clast lithologies in the Harricana complex.

The timing here is critical. Streamlined landforms were formed before the cross-cutting striations. Their orientation was not affected by later SSE ice flow. Consequently, they could not have been formed incrementally under the influence of local flow conditions. Rather, they give a synoptic view of coherent flow over a broad region (Fig. 20).

Reestablishment of an integrated subglacial drainage system, directed by hydraulic gradients towards the trunk conduit, accounts for the convergence of large eskers on the Harricana complex (Fig. 1). With a continuous trunk conduit in

place, it is a simple matter to imagine sediment transport in a conduit of variable geometry, deposition of sediment by extremely high energy flows, and unsteady flow varying with weather, seasonal changes or changes in the drainage system (Fig. 21C). This combination of conduit and flow characteristics accounts for the morphology of the complex, its clast lithologies and roundness, and the gravel facies and macroforms it contains.

With ice wasting and transgression of large, ice-dammed lakes south of the dwindling ice sheet, calving, formation of embayments, and deposition of fans over conduit deposits where the ice sheet was thin were probable.

The cause of the apparent change in geometry of the ice sheet in this region, prior to 11 ka BP is an open question (cf. Dyke and Prest, 1987). There appears to be three possible answers: (i) the geometry was a product of earlier convergence of two separate ice masses (cf. Dyke et al., 1982); (ii) it resulted from downdraw driven by subglacial deformation and consequent higher flow rates in the Great Lakes region (Veillette, 1986, 1990); or (iii) it was the result of a meltwater-flood event. For the Harricana complex, suggestion (i) cannot be substantiated (Table 7) (Veillette, 1986). The second suggestion requires pervasive deformation near the southern margin of the Laurentide Ice Sheet to have triggered downdraw, and implies time-transgressive formation of the suture and of the Harricana complex. Our research favours synchronous formation of, at least, the eskerine core of the studied portion of the Harricana complex, perhaps with later, superimposed, grounding-line sedimentation. The location of the complex is interpreted to have been determined by regional-scale convergence within a meltwater-sheet flow. This convergence may have been a result of flow being funnelled through the highly dissected part of the Abitibi Uplands to the south (Figs. 1, 20). Development of a deglacial corridor along the Harricana complex axis is readily explained by thinner ice over a large subglacial conduit. Our observations favour synchronous regional changes in ice-sheet geometry related to the effects of a meltwater-flood event.

Acknowledgements

This research was funded by a Canadian Commonwealth Scholarship to TAB, and a NSERC Canada operating grant to JS. Field assistance was ably given by Colin Booth. John Glew and Michael Fisher drafted Figs. 17, 20 and 21. Randy Pakan, David Epp and Graham Wiley printed the figures. We thank Jean Veillette (GSC) for initially provoking our interest in the Harricana complex and adjacent landforms and sediments, and for providing constructive comments on an early version of this manuscript. Comments by reviewers G.F. Dardis and A.J. van Loon were appreciated.

References

Aario, R., 1977. Classification and terminology of morainic landforms in Finland. Boreas, 6: 87–100.

Allard, M., 1974. Géomorphologie des eskers Abitibiens. Cah. Géogr. Québec, 18: 271–296.

Allen, J.R.L., 1984. Sedimentary Structures: Their Character and Physical Basis. Developments in Sedimentology 30, Vol. 1, Elsevier, Amsterdam, 593 pp.

Ashmore, P.E., 1991. How do gravel rivers braid? Can. J. Earth Sci., 28: 326–341.

Baker, V.R., 1978. Large-scale erosional and depositional features of the Channeled Scabland. In: V.R. Baker and D. Nummedal (Editors), The Channeled Scabland: A Guide to the Geomorphology of the Columbia Basin, Washington. National Aeronautics and Space Administration, Washington, pp. 81–115.

Banerjee, I. and McDonald, B.C., 1975. Nature of esker sedimentation. In: A.V. Jopling and B.C. McDonald (Editors), Glaciofluvial and Glaciolacustrine Sedimentation. Soc. Econ. Paleontol. Mineral., Spec. Publ., 23: 304–320.

Boissonneau, A.N., 1968. Glacial history of northeastern Ontario, II. The Timiskaming–Algoma area. Can. J. Earth Sci., 5: 97–109.

Brayshaw, A.C., 1984. Bed microtopography and entrainment thresholds in gravel-bed rivers. Geol. Soc. Am. Bull., 96: 218–233.

Brennand, T.A., 1993. Laurentide Meltwater Systems: Geomorphic and Sedimentary Evidence. Ph.D. thesis, University of Alberta, Edmonton.

Brennand, T.A., 1994. Macroforms, large bedforms and rhythmic sedimentary sequences in subglacial eskers, south-central Ontario: implications for esker genesis and meltwater regime. Sediment. Geol., 91: 9–55.

Brennand, T.A. and Sharpe, D.R., 1993. Ice-sheet dynamics and subglacial meltwater regime inferred from form and sedimentology of glaciofluvial systems: Victoria Island, District of Franklin, Northwest Territories. Can. J. Earth Sci., 30: 928–944.

Brennand, T.A. and Shaw, J., 1994. Tunnel channels and associated landforms, south-central Ontario: their implications for ice-sheet hydrology. Can. J. Earth Sci., 31: 505–522.

Chauvin, L., 1977. Géologie des dépôts meubles de la région de Joutel–Matagami. Ministère des Richesses Naturelles, dossier public 539, 106 pp.

Cheel, R.J., 1982. The depositional history of an esker near Ottawa, Canada. Can. J. Earth Sci., 19: 1417–1427.

Cheel, R.J., 1990. Horizontal lamination and the sequence of bed phases and stratification under upper flow regime conditions. Sedimentology, 37: 517–529.

Cheel, R.J. and Middleton, G.V., 1986. Horizontal laminae formed under upper flow regime plane bed conditions. J. Geol., 94: 489–504.

Costa, J.E., 1988. Rheologic, geomorphologic, and sedimentologic differentiation of water floods, hyperconcentrated flows, and debris flows. In: V.R. Baker, R.C. Koche, and P.C. Patton (Editors), Flood Geomorphology. John Wiley and Sons, London, pp. 113–122.

Curray, J.R., 1956. The analysis of two-dimensional orientation data. J. Geol., 64: 177–131.

Davis, J.C., 1986. Statistical and Data Analysis in Geology, 2nd ed. John Wiley and Sons, New York, 646 pp.

De Geer, G., 1897. Om rullstensåsarnas bildningssätt. Geol. Fören. Stockholm Förh., 19: 366–388.

Dredge, L.A. and Cowan, W.R., 1989. Quaternary geology of the southwestern Canadian Shield. In: R.J. Fulton (Editor), Quaternary Geology of Canada and Greenland. Geological Survey of Canada, Geology of Canada, No. 1, pp. 214–249.

Duckworth, P.B., 1979. The late depositional history of the western end of the Oak Ridges Moraine, Ontario. Can. J. Earth Sci., 16: 1094–1107.

Dyke, A.S. and Prest, V.K., 1987. Late Wisconsinan and Holocene history of the Laurentide Ice Sheet. Géogr. Phys. Quat., 41: 237–263.

Dyke, A.S., Dredge, L.A. and Vincent, J.-S., 1982. Configuration and dynamics of the Laurentide Ice Sheet during the Late Wisconsin maximum. Géogr. Phys. Quat., 36: 5–14.

Elfström, Å., 1987. Large boulder deposits and catastrophic floods: a case study of the Båldkatj area, Swedish Lapland. Geogr. Ann., Ser. A, 69: 101–121.

Fisher, R.V., 1990. Transport and deposition of a pyroclastic surge across an area of high relief: the 18 May 1980 eruption of Mount St. Helens, Washington. Geol. Soc. Am. Bull., 102: 1038–1054.

Fraser, G.S. and Bleuer, N.K., 1988. Sedimentological consequences of two floods of extreme magnitude in the late Wisconsinan Wabash Valley. Geol. Soc. Am., Spec. Pap., 229: 111–125.

Gorrell, G. and Shaw, J., 1991. Deposition in an esker, bead and fan complex, Lanark, Ontario, Canada. Sediment. Geol., 72: 285–314.

Hardy, L., 1976. Contribution à l'étude géomorphologique de la portion québécoise des basses terres de la baie de James. Thèse de doctorat, Université McGill, Montréal.

Hardy, L., 1977. La déglaciation et les épisodes lacustre et marin sur le versant québécois des basses terres de la Baie de James. Géogr. Phys. Quat., 31: 261–273.

Hardy, L., 1982. Le Wisconsinien supérieur à l'est de la Baie James (Québec). Nat. Can., 109: 333–351.

Heikkinen, O. and Tikkanen, M., 1989. Drumlins and flutings in Finland: their relationships to ice movement and to each other. Sediment. Geol., 62: 349–355.

Hicock, S.R. and Dreimanis, A., 1992. Deformation till in the Great Lakes region: implications for rapid flow along the south-central margin of the Laurentide Ice Sheet. Can. J. Earth Sci., 29: 1565–1579.

Hooke, R. LeB., 1989. Englacial and subglacial hydrology: a qualitative review. Arct. Alp. Res., 21: 221–233.

Iken, A. and Bindshadler, R.A., 1986. Combined measurements of subglacial and surface velocity of Findelengletscher, Switzerland: conclusions about drainage system and sliding mechanism. J. Glaciol., 32: 101–119.

Iseya, F. and Ikeda, H., 1987. Pulsations in bedload transport rates induced by longitudinal sediment sorting: a flume study using sand and gravel mixtures. Geogr. Ann., Ser. A, 69: 15–27.

Jaeggi, M.N.R., 1984. Formation and effects of alternate bars. ASCE J. Hydraul. Eng., 110: 142–156.

Johansson, C.E., 1976. Structural studies of frictional sediments. Geogr. Ann., 58: 201–300.

Kaszycki, C.A. and DiLabio, R.N.W., 1986. Surficial geology and till geochemistry, Llyn Lake–Leaf Rapids region, Manitoba. In: Current Research, Part B. Geol. Surv. Can., Pap. 86-1B, pp. 245–256.

Kor, P.S.G., Shaw, J. and Sharpe, D.R., 1991. Erosion by subglacial meltwater, Georgian Bay, Ontario: a regional view. Can. J. Earth Sci., 28: 623–642.

Low, A.P., 1888. Report on explorations in James' Bay and country east of Hudson Bay, drained by the Big, Great Whale and Clearwater rivers. Geol. Surv. Can., Annu. Rep., 3(2-J): 1J–94J.

McClenaghan, M.B., 1989. Quaternary Geology and Geochemical Exploration in the Matheson Area, Northeastern Ontario. M.Sc. Thesis, Queen's University, Kingston.

McClenaghan, M.B., Lavin, O.P., Nichol, I. and Shaw, J., 1988. Quaternary geology and geochemical exploration in the Matheson area, northeastern Ontario. In: D.R. MacDonald and K.A. Mills (Editors), Prospecting in Areas of Glaciated Terrain–1988. Canadian Institute of Mining and Metallurgy, pp. 1–20.

McClenaghan, M.B., Lavin, O.P., Nichol, I. and Shaw, J., 1992. Geochemistry and clast lithology as an aid to till classification, Matheson, Ontario, Canada. J. Geochem. Explor., 42: 237–260.

McDonald, B.C. and Shilts, W.W., 1975. Interpretation of faults in glaciofluvial sediments. In: A.V. Jopling and B.C.

McDonald (Editors), Glaciofluvial and Glaciolacustrine Sedimentation. Soc. Econ. Paleontol. Mineralogists, Spec. Publ., 23: 123–131.

McDonald, B.C. and Vincent, J.S., 1972. Fluvial sedimentary structures formed experimentally in a pipe, and their implications for interpretation of subglacial sedimentary environments. Geol. Surv. Can., Pap. 72-27.

Meland, N. and Norrman, J.O., 1969. Transport velocities of individual size fractions in heterogeneous bed load. Geogr. Ann., Ser. A, 51: 127–144.

MERQ-OGS, 1983. Lithostratigraphic map of the Abitibi Subprovince. Ontario Geological Survey/Ministère de l'Énergie et des Ressources, Québec, 1:500,000. Catalogued as "Map 2484" in Ontario and "DV 83-16" in Québec.

Miall, A.D., 1985. Architectural-element analysis: a new method of facies analysis applied to fluvial deposits. Earth Sci. Rev., 22: 261–308.

Paterson, W.S.B., 1981. The Physics of Glaciers. Pergamon, Oxford, 380 pp.

Pierson, T.C. and Scott, K.M,. 1985. Downstream dilution of a lahar: transition from debris flow to hyperconcentrated streamflow. Water Resour. Res., 21: 1511–1542.

Postma, G., Nemec, W. and Kleinspehn, K.L., 1988. Large floating clasts in turbidites: a mechanism for their emplacement. Sediment. Geol., 58: 47–61.

Powers, M.C., 1953. A new roundness scale for sedimentary particles. J. Sediment. Petrol., 23: 117–119.

Prest, V.K., Grant, D.R. and Rampton, N., 1968. Glacial Map of Canada. Geological Survey of Canada Map 1253A, scale 1:5,000,000.

Punkari, M., 1980. The ice lobes of the Scandinavian Ice Sheet during the deglaciation in Finland. Boreas, 9: 307–310.

Punkari, M., 1985. Glacial geomorphology and dynamics in Soviet Karelia interpreted by means of satellite imagery. Fennia, 163: 113–153.

Richard, P.J.H., Veillette, J.J. and Larouche, A.C., 1989. Palynostratigraphie et chronologie du retrait glaciaire au Témiscamingue: évaluation des âges ^{14}C et implications paléoenvironmentales. Can. J. Earth Sci., 26: 627–641.

Ringrose, S., 1982. Depositional processes in the development of eskers in Manitoba. In: R. Davidson-Arnott, W. Nickling and B.D. Fahey (Editors), Research in Glacial, Glaciofluvial and Glaciolacustrine Systems. Proc. 6th Guelph Symp. Geomorphology. Geo-Books, Norwich, pp. 117–137.

Röthlisberger, H., 1972. Water pressure in intra and subglacial channels. J. Glaciol., 11: 177–203.

Rouse, H., 1961. Fluid Mechanics for Hydraulic Engineers. Dover Publications Inc., New York, 422 pp.

Rust, B.R., 1972. Pebble orientation in fluvial sediments. J. Sediment. Petrol., 42: 384–388.

Rust, B.R., 1984. Proximal braidplain deposits in the Middle Devonian Malbaie Formation of Eastern Gaspé, Quebec, Canada. Sedimentology, 31: 675–695.

Rust, B.R. and Koster, E.H., 1984. Coarse alluvial deposits. In: R.G. Walker (Editor), Facies Models, 2nd ed. Geoscience Canada Reprint Series 1, Toronto, pp. 53–69.

Sado, E.V. and Carswell, B.F., 1987. Surficial Geology of Northern Ontario. Ontario Geological Survey Map 2518, scale 1:1,200,000.

Shaw, J., 1972. Sedimentation in the ice-contact environment, with examples from Shropshire (England). Sedimentology, 18: 23–62.

Shaw, J., 1994. A qualitative view of sub-ice-sheet landscape evolution. Progr. Phys. Geogr., 18: 159–184.

Shaw, J. and Gorrell, G., 1991. Subglacially formed dunes with bimodal and graded gravel in the Trenton drumlin field, Ontario. Géogr. Phys. Quat., 45: 21–34.

Shaw, J. and Kellerhals, R., 1977. Paleohydraulic interpretation of antidune bedforms with application to antidunes in gravel. J. Sediment. Petrol., 47: 257–266.

Shaw, J. and Kellerhals, R., 1982. The composition of recent alluvial gravels in Alberta river beds. Alta. Geol. Surv., Bull., 41, 151 pp.

Shaw, J., Kvill, D. and Rains, B., 1989. Drumlins and catastrophic subglacial floods. Sediment. Geol., 62: 177–202.

Shilts, W.W. and Wyatt, P.H., 1988. Aminostratigraphy of marine and associated nonglacial beds of the Hudson Bay Lowland. In: Institute of Arctic and Alpine Research, 17th Annual Workshop, University of Colorado, Boulder, Abstracts, p. 49.

Shilts, W.W., Aylsworth, J.M., Kaszycki, C.A. and Klassen, R.A., 1987. Canadian Shield. In: W.L. Graf (Editor), Geomorphic Systems of North America. Geol. Soc. Am., Centennial Spec. Vol., 2: 119–161.

Shoemaker, E.M., 1992. Water sheet outburst floods from the Laurentide Ice Sheet. Can. J. Earth Sci., 29: 1250–1264.

Shreve, R.L., 1972. Movement of water in glaciers. J. Glaciol., 11: 205–214.

Shreve, R.L., 1985. Esker characteristics in terms of glacial physics, Katahdin esker system, Maine. Geol. Soc. Am. Bull., 96: 639–646.

Skinner, R.G., 1973. Quaternary stratigraphy of the Moose River Basin, Ontario. Geol. Surv. Can., Bull., 225.

Skipper, K., 1971. Antidune cross-stratification in a turbidite sequence, Chloridorme Formation, Gaspé, Québec. Sedimentology, 17: 51–68.

Smith, G.A., 1986. Coarse-grained nonmarine volcaniclastic sediment: terminology and depositional process. Geol. Soc. Am. Bull., 97: 1–10.

Smith, S.A., 1990. The sedimentology and accretionary styles of an ancient gravel-bed stream: the Budleigh Salterton Pebble Beds (Lower Triassic), southwest England. Sediment. Geol., 67: 199–219.

Smith, S.L., 1992. Quaternary stratigraphic drilling transect, Timmins to the Moose River Basin, Ontario. Geol. Surv. Can., Bull., 415, 94 pp.

Sneed, E.D. and Folk, R.L., 1958. Pebbles in the lower Colorado River, Texas: a study in particle morphogenesis. J. Geol., 66: 114–150.

Steele, K.G., Baker, C.L. and McClenaghan, M.B., 1989. Models of glacial stratigraphy determined from drill core,

Matheson area, northeastern Ontario. In: R.N.W. DiLabio and W.B. Coker (Editors), Drift Prospecting. Geol. Surv. Can., Pap., 89-20: 127–138.

Thorleifson, L.H., Wyatt, P.H., Shilts, W.W. and Nielsen, E., 1992. Hudson Bay lowland Quaternary stratigraphy: evidence for early Wisconsinan glaciation centred in Quebec. In: P.U. Clark and P.D. Lea (Editors), The Last Interglacial–Glacial Transition in North America. Geol. Soc. Am., Spec. Pap., 270: 207–221.

Thorleifson, L.H., Wyatt, P.H. and Warman, T.A., 1993. Quaternary stratigraphy of the Severn and Winsk drainage basins, Northern Ontario. Geol. Surv. Can., Bull., 442.

Tremblay, G., 1974. Géologie du Quaternaire, régions de Rouyn–Noranda et d'Abitibi, comtés d'Abitibi-est et d'Abitibi-ouest, Québec. Ministère des Richesses Naturelles, dossier public 236.

Tremblay, L.P., 1950. Piedmont map area, Abitibi county, Quebec. Geol. Surv. Can., Mem., 253.

Veillette, J.J., 1983. Déglaciation de la vallée supérieure de l'Outaouais, le lac Barlow et le sud de lac Ojibway, Québec. Géogr. Phys. Quat., 37: 67–84.

Veillette, J.J., 1986. Former ice flows in the Abitibi–Timiskaming region: implications for the configuration of the late Wisconsinan ice sheet. Can. J. Earth Sci., 23: 1724–1741.

Veillette, J.J., 1988. Déglaciation et évolution des lacs proglaciaires post-Algonquin et Barlow au Témiscaningue, Québec et Ontario. Géogr. Phys. Quat., 42: 7–31.

Veillette, J.J., 1989. Ice movements, till sheets and glacial transport in Abitibi–Timiskaming, Quebec and Ontario. In: R.N.W. DiLabio and W.B. Coker (Editors), Drift Prospecting. Geol. Surv. Can., Pap., 89-20: 139–154.

Veillette, J.J., 1990. Le Dernier Glaciaire au Témagamingue, Québec et Ontario. Thèse de doctorat, Université Libre de Bruxelles.

Veillette, J.J., Averill, S.A., LaSalle, P. and Vincent, J.-S., 1989. Quaternary Geology of Abitibi–Témiscamingue and Mineral Exploration. Field Trip B1 of the Geological Association of Canada, Guidebook, 122 pp.

Veillette, J.J., Paradis, S.J., Thibaudeau, P. and Pomares, J.-S., 1991. Distribution of distinctive Hudson Bay erratics and the problem of the Cochrane limit in Abitibi, Quebec. In: Current Research, Part C. Geol. Surv. Can., Pap., 91-1C: 135–142.

Vincent, J.-S., 1989. Quaternary geology of the southeastern Canadian Shield. In: R.J. Fulton (Editor), Quaternary Geology of Canada and Greenland. Geological Survey of Canada, Geology of Canada, No. 1, pp. 249–274.

Vincent, J.-S. and Hardy, L., 1979. The evolution of glacial lakes Barlow and Ojibway, Quebec and Ontario. Geol. Surv. Can., Bull., 316.

Walder, J. and Hallet, B.H., 1979. Geometry of former subglacial water channels and cavities. J. Glaciol., 23: 335–346.

Williams, G.P. 1983. Paleohydrological methods and some examples from Swedish fluvial environments. Geogr. Ann., Ser. A, 65: 227–243.

Wilson, J.T., 1938. Glacial geology of part of north-western Quebec. Transactions of the Royal Society of Canada, Section 4, 32: 49–59.

Woodcock, N.H. and Naylor, M.A., 1983. Randomness testing in three-dimensional orientation data. J. Struct. Geol., 5: 539–548.

Wright, H.E. Jr., 1973. Tunnel valleys, glacial surges and subglacial hydrology of the Superior lobe, Minnesota. In: R.F. Black, R.P. Goldthwaite and H.B. Willman (Editors), The Wisconsinan Stage. Geol. Soc. Am., Mem., 136: 251–276.

Yelle, J.S., 1976. Physiographic Map of Eastern Canada and Adjacent Areas. Geological Survey of Canada, Map 1399A (SW), scale 1:2,000,000.